REPORT DOCUMENTATION PAGE

Form Approved
OMB NO. 0704-0188

Public Reporting burden for this collection of information is estimated to average 1 hour per response, including the time for reviewing instructions, searching existing data sources, gathering and maintaining the data needed, and completing and reviewing the collection of information. Send comment regarding this burden estimates or any other aspect of this collection of information, including suggestions for reducing this burden, to Washington Headquarters Services, Directorate for information Operations and Reports, 1215 Jefferson Davis Highway, Suite 1204, Arlington, VA 22202-4302, and to the Office of Management and Budget, Paperwork Reduction Project (0704-0188,) Washington, DC 20503.

1. AGENCY USE ONLY (Leave Blank)	2. REPORT DATE	3. REPORT TYPE AND DATES COVERED
	March 15, 2007	Final Report: Oct 1, 2005 - Oct 1, 2006

4. TITLE AND SUBTITLE
Rapid Vaccine Manufacturing Facility: Emerging Pathogen Countermeasure Response. Initial Proof of Concept Stage

5. FUNDING NUMBERS
W911NF-05-1-0545

6. AUTHOR(S)
Adrian Vilalta, Edward Domanico, Jennifer Chaplin

7. PERFORMING ORGANIZATION NAME(S) AND ADDRESS(ES)
Vical Incorporated, 10390 Pacific Center Ct., San Diego, CA 92121

8. PERFORMING ORGANIZATION REPORT NUMBER
DARPA POC Final Report 070315

9. SPONSORING / MONITORING AGENCY NAME(S) AND ADDRESS(ES)
U. S. Army Research Office
P.O. Box 12211
Research Triangle Park, NC 27709-2211

10. SPONSORING / MONITORING AGENCY REPORT NUMBER
49426.1-LS-DRP

11. SUPPLEMENTARY NOTES
The views, opinions and/or findings contained in this report are those of the author(s) and should not be construed as an official Department of the Army position, policy or decision, unless so designated by other documentation.

12 a. DISTRIBUTION / AVAILABILITY STATEMENT
Approved for public release; distribution unlimited.

12 b. DISTRIBUTION CODE

13. ABSTRACT (Maximum 200 words)

Initial feasibility of using PCR-generated DNA vaccines (LEC) was completed as outlined in our proposal of July 21, 05. Specifically we demonstrated that (a) manufacture of milligram amounts of LEC DNA vaccine against H3N2 and H1N1 influenza strains was possible using microplate PCR technology; (b) resulting LEC DNA could be purified and formulated with the cationic lipid delivery system Vaxfectin and (c) vaccination of mice with Vaxfectin-formulated LEC vaccine resulted in protection against a lethal viral challenge. In addition, objectives outlined in our Expanded Aims proposal of Feb 21, 06 were met. Specifically, we compared the performance of LEC vaccination to that of pDNA vaccination using the mouse influenza challenge model. These data indicate that Vaxfectin-formulated pDNA outperformed Vaxfectin-formulated LEC at doses between 0.4 and 0.08 ug. Protection data for pDNA vs. LEC at doses 2 ug or above were statistically indistinguishable. We also evaluated one potential scalable PCR device concept. Heat transfer characteristics of materials and fluids were determined and PCR amplification was attempted at the 10 and 100 mL reaction volumes. Although DNA amplification was unsuccessful, causes for this outcome were identified and potential solutions have been proposed.

14. SUBJECT TERMS
Polymerase Chain Reaction (PCR); Linear Expression Cassette (LEC); DNA vaccine; Influenza; Pathogen Countermeasure Response; Amplicon; Vaccination

15. NUMBER OF PAGES
68

16. PRICE CODE

17. SECURITY CLASSIFICATION OR REPORT	18. SECURITY CLASSIFICATION ON THIS PAGE	19. SECURITY CLASSIFICATION OF ABSTRACT	20. LIMITATION OF ABSTRACT
UNCLASSIFIED	UNCLASSIFIED	UNCLASSIFIED	UL

NSN 7540-01-280-5500

Standard Form 298 (Rev.2-89)
Prescribed by ANSI Std. 239-18
298-102

1. Table of Contents

2. List of Appendices

Appendix I: cfPCR Reactor Design Evaluation.

Appendix II: Draft of manuscript: "Vaccination with PCR-generated Linear Expression Cassettes protects Mice against Lethal Influenza A Challenge" by Adrián Vilalta, Gretchen Jimenez, Denis Rusalov, Peggy Lalor, Kristin Carner, Jennifer A. Chaplin, Michael Komai, Marston Manthorpe and David C. Kaslow

3. Statement of the Problem Studied

Feasibility of using PCR to generate effective DNA vaccines was explored.

4. Summary of Most Important Results

Data generated under this grant demonstrated that vaccination with influenza A HA-expressing LEC DNA can protect BALB/c mice against a lethal dose of influenza A. LEC DNA was produced through a small-scale PCR process using both phosphodiester and phosphorothioate-modified oligonucleotide primers. Unformulated LEC DNA was shown to protect mice against viral challenge. In addition, high levels of protection were observed using lower doses of LEC DNA when formulated with the cationic lipid system Vaxfectin™. It was demonstrated that PCR amplification can produce LEC DNA within a few hours; purification and formulation of the resulting DNA only required an additional day. In contrast, production of pDNA through conventional bacterial fermentation followed by cell lysis and chromatography would typically require a minimum of 7 days.

LECs for the Phase 1 investigation were synthesized in 96-well plates in order to establish Proof of Principle. The next phase of investigation will require the development of a reactor for larger scale production. This grant covered two main activities geared to the evaluation of a continuous flow PCR device, specifically (a) heat transfer of materials and fluids and (b) construction of a small scalable continuous flow PCR (cfPCR) device were carried out. DNA amplification was attempted unsuccessfully using the small cfPCR device.

5. List of Publications supported under the Grant

i. Papers presented at Meetings

Paper entitled "Vaccination with Linear Expression Cassettes protects Mice against Lethal Influenza A Challenge" will be presented at the 2007 American Society of Gene Therapy.

ii. Manuscripts submitted for publication

Manuscript entitled "Vaccination with PCR-generated Linear Expression Cassettes protects Mice against Lethal Influenza A Challenge" was submitted to *Human Gene Therapy* for review on Jan07. Authors: Adrián Vilalta, Gretchen Jimenez, Denis Rusalov, Peggy Lalor, Kristin Carner, Jennifer A. Chaplin, Michael Komai, Marston Manthorpe and David C. Kaslow.

i. Technical reports submitted to ARO

Quarterly reports were submitted on 20Jan06 and 21Feb06.

6. Report of Inventions

Patent application entitled "Linear Expression Cassette Vaccines" was submitted to the USPTO on Dec06. Inventors: Adrián Vilalta, Denis Rusalov, Ed Domanico, Amit Vasvada, Marston Manthorpe, David C. Kaslow and Alain Rolland. Pat App #60,868,496.

7. Expanded Aims Report

Results from studies initially described on our expanded aims proposal (21Feb06) are presented below. Data for studies carried out between Jan 20 and Feb 21, 2006 have been provided in report DARPA POC Q1Update Report 060120.

Dose Response Studies

Our previous mouse influenza challenge experiments established the ability of Linear Expression Cassette LEC DNA (LEC) to function as a vaccine. LECs expressing Hemagglutinin H3 (LEC_{HAH3}) are able to provide 100% protection from lethal challenge with a single injection of 40 µg of LEC_{HAH3} in PBS or as little as 2 µg $LEC_{MOD\text{-}HAH3}$ (modified oligonucleotides) formulated in Vaxfectin™. The follow up mouse challenge study allowed us to explore the following:

1) Do LECs and plasmid DNA provide equivalent levels of protection on a molar basis?

2) Does Vaxfectin™ formulation provide added protective value to the LEC-based vaccine?

We addressed the levels of protection provided by decreasing doses of HAH3 pDNA in a dose ranging study for another Vical program. This was essential to establish the appropriate dose for comparing pDNA vs. LEC. In addition, we explored the contribution of the cationic lipid Vaxfectin™ at extremely low pDNA levels. These data were used to finalize the doses included in the experiment below.

Protocol:

In our LEC dosing study, we compared pDNA vs. LEC generated with modified oligonucleotides ($LEC_{MOD\text{-}HAH3}$); both types of DNA express influenza HAH3 antigen. We compared two doses of VR4750 (HAH3-expressing pDNA) in PBS with two doses of LEC $_{MOD\text{-}HAH3}$, either in PBS or Vaxfectin™ -formulated. This allowed us to compare pDNA vs. LEC, as well as the contribution of Vaxfectin™ formulation to $LEC_{MOD\text{-}HAH3}$ survival. Mice received a single vaccination of LEC_{HAH3} or pDNA and were challenged with virus six weeks after the vaccination. A 50 µg dose of VR4750 served as the positive control; PBS served as the negative control.

The primary endpoint in this experiment was survival (protection); body mass loss was used as a secondary endpoint.

Study Design:

We utilized half the mass in the LEC groups in order to use equimolar amounts of HAH3 open reading frames compared to pDNA. The 2 µg Vaxfectin™ -formulated LEC $_{MOD\text{-}HAH3}$ group provided a bridge to our second LEC challenge experiment (see 1st Quarterly Report Update, 21Feb06).

Table 1 Study Design

Group	DNA	Dose	Formulation	# mice
A	VR4750	10 µg	Vaxfectin™	10
B	VR4750	0.4 µg	PBS	12
C	VR4750	0.4 µg	Vaxfectin™	12
D	VR4750	0.08 µg	Vaxfectin™	12
E	$LEC_{MOD\text{-}HAH3}$	2 µg	Vaxfectin™	12
F	$LEC_{MOD\text{-}HAH3}$	0.2 µg	Vaxfectin™	12
G	$LEC_{MOD\text{-}HAH3}$	0.2 µg	PBS	12
H	$LEC_{MOD\text{-}HAH3}$	0.04 µg	Vaxfectin™	12
I	$LEC_{MOD\text{-}HAH3}$	0.04 µg	PBS	12
J	PBS (neg control)	N/A	N/A	10

Results:

Survival data for the study are summarized in Figure 1. Data indicate that mice are 100% protected against lethal viral challenge when vaccinated with as little as 0.4 µg of Vaxfectin™-formulated HAH3 pDNA; partial protection (~40% survival) was observed in mice vaccinated with 0.08 µg of the Vaxfectin™-formulated pDNA vaccine. No animals survived the challenge when vaccinated with 0.4 µg of the pDNA in PBS P=0.01). Mice in the 0.4 µg pDNA Vaxfectin™-formulated group lost an average of 9% of their body weight by Day 6 post-challenge, while the 0.4 µg PBS group had lost >20% of their body weight (data not shown). Compared to HAH3 pDNA in PBS, Vaxfectin™ formulation provided an approximately 5-fold dose-sparing effect. In contrast, mice vaccinated with less than 2 µg of HAH3 LEC did not survive the challenge irrespective of the formulation used. These data suggest that although LEC DNA can successfully vaccinate mice against the mouse adapted flu strain, larger molar doses might be needed as compared to pDNA. These results indicate that future investigations on LEC structure-stability might be required to bring LEC potency on a par with pDNA vaccines.

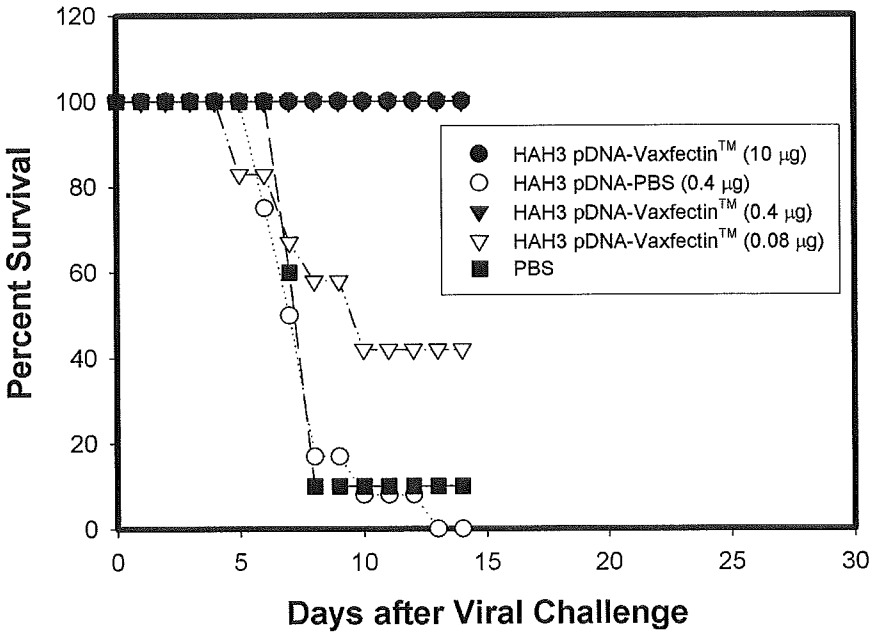
120
100
80
60
40
20
0
Percent Survival
0
5
10
15
20
25
30
Days after Viral Challenge
HAH3 pDNA-Vaxfectin™ (10 μg)
HAH3 pDNA-PBS (0.4 μg)
HAH3 pDNA-Vaxfectin™ (0.4 μg)
HAH3 pDNA-Vaxfectin™ (0.08 μg)
PBS

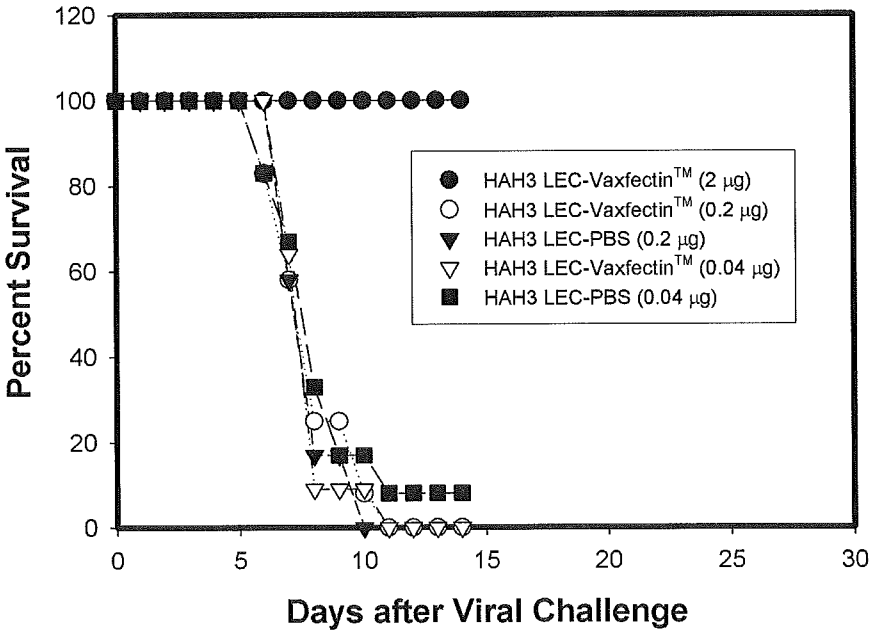
120
100
80
60
40
20
0
Percent Survival
0
5
10
15
20
25
30
Days after Viral Challenge
HAH3 LEC-Vaxfectin™ (2 μg)
HAH3 LEC-Vaxfectin™ (0.2 μg)
HAH3 LEC-PBS (0.2 μg)
HAH3 LEC-Vaxfectin™ (0.04 μg)
HAH3 LEC-PBS (0.04 μg)

Figure 1.

Reactor Design-Evaluation

Evaluation of continuous-flow PCR reactor first proposed on our 21Feb06 proposal is described in detail in Appendix I.

Costs

Actual expenditures are shown in the following spreadsheet. The official amount of $500,000 was spent in June 2006.

GRANT STATUS REPORT (LIFE-TO-DATE)

FOR GRANT PERIOD JULY 1, 2005 THROUGH SEPTEMBER 30, 2006

VICAL INCORPORATED
Confidential - For Internal Use Only
Period: SEPTEMBER-06 currency USD
Submitted: 18-OCT-06 15:40:48

PROJ=G04005 (DARPA cPCR GRANT)

	Incurred YTD 2005 (Beg. 7/01/05)	Incurred YTD 2006	Incurred Total	Grant Budget	Amount (Over)/ Under Budget	% Incurred to Budget
Revenue Recognized (See note)#	274,543	225,059	500,002	500,000	(2)	100.00%
Contract Services	1,743	3,478	5,221	0	(5,221)	
Internal Travel	0	0	0	0	0	
Supplies	52,939	42,572	95,511	75,947	(19,564)	
Other	0	31	31	0	(31)	
Direct Labor $ (See note)+	59,937	58,117	118,054	116,819	(1,235)	
Temp Labor $ (See note)+	107	0	107	0	(107)	
Fringe (Adjusted Gov't Rate)*	10,789	10,461	21,250	21,027	(223)	
Overhead (Adjusted Gov't Rate)*	147,108	142,386	289,494	286,287	(3,207)	
Total Expense	272,623	257,045	529,668	500,000	(29,668)	105.93%
Direct Labor Hours (See note)+	1671.25	1,556	3,227	2600.00	(627)	
Temp Labor Hours (See note)+	4.00	0	4	0.00	(4)	
Total Labor Hours	1675.25	1556.00	3231.25	2600.00	(631.25)	124.28%
Labor Cost Per Hour	$35.84	$37.35	$36.67	$44.93		

(#) Revenue Recognized has not been reduced by NIH reserve allowance on this report.

(+) Direct and Temp Labor $ and Hours include actual hrs. x actual rates for all personnel (no allocated amounts); Rates have been adjusted to reflect uncompensated overtime for exempt employees.

(*) Allowable government rates for this grant are 18.00% for Fringe, 246.00% for Overhead; Fringe is not applied to Temp Labor.

Appendix I cfPCR REACTOR DESIGN EVALUATION

1. Introduction

The following (1) heat transfer studies and (2) construction of a small scalable continuous flow PCR device described in our proposal for use of remaining funds on PCR DARPA Phase 1 grant is complete. The results are presented below.

1.1 Heat Transfer Testing of Materials and Fluids

The design of a scaleable Polymerase Chain Reaction (PCR) device configured to produce pharmaceutical grade material was constructed of both Teflon® (PTFE) and 316L stainless steel. As such, these materials were configured to allow for testing and determination of the heat transfer characteristics associated with the design of a system that can produce the rapid controlled change of processing temperatures as PCR cycles are completed on a test fluid. This work completed experiments that lead to the construction of a mathematical model capable of predicting the heat transfer performance of available materials and fluids used to design such a system.

2. Experimental Determination of Heat Transfer Characteristics

The PCR reactors were designed to use Finnzymes *Detergent-free Phusion ™ HF Buffer*, "Buffer", *2X Phusion ™ HF Master Mix*, "Master Mix", and *Phusion™ High-Fidelity DNA Polymerase* "Enzyme". A literature search was performed to determine chemical composition of each of the reactor "fluids". It was determined that the major constituent of each of the components is water. Therefore, the physical properties for all the reactor fluids were assumed to be very similar to each other and also to water. Viscosities, densities, specific heats, and thermal conductivities of water at each section temperature were determined as in Table 2.1.

Heat Transfer Properties Used for all Reactor Fluids

Section	Sect T (C)	Viscosity μ kg/(m*s)	Density ρ (kg/m^3)	Specific Heat C_p (J/kgK)	Thermal Conductivity k (W/m*K)
HX1	85	3.28E-04	967	4202	0.666
HOLD1	98	2.88E-04	962	4214	0.672
HX2	74	3.85E-04	975	4193	0.660
HOLD2	50	5.49E-04	989	4181	0.648
HX3	61	4.66E-04	980	4186	0.654
HOLD3	72	3.97E-04	977	4192	0.659

Table 2.1

2.1 Thermal conductivity of materials of construction

The reactor tubing materials were constructed of Teflon™, "PTFE" and 316L stainless steel, "316L". The thermal conductivities for each of these materials were determined from literature. See table 2.2.

Thermal Conductivities of Materials of Construction

PTFE	316L
Thermal Conductivity *k* (W/m*K)	Thermal Conductivity *k* (W/m*K)
0.25	17

Table 2.2

3. Design, Construction, and Testing of a PCR Reactor

The model was developed through (1) the experimental determination of heat transfer characteristics used to predict the scale-up and (2) the configuration of a simple single pass heat exchanger test device (HETD) in order to determine the accuracy of predictions for a 400 mL (total volume) reactor scale.

3.1 Assumptions

The following assumptions were made in the design of the HETD and PCR reactor. The overall assumptions made were that the physical properties of the Buffer, Master Mix, and Enzyme were assumed to be similar to that of water.

3.1.1 Tubing Size Determination

The initial small scale design hold-up volume was 40mL. Very small inside diameter (ID) tubing was initially designed to accommodate the 40mL. The length of small ID tubing required to achieve the hold time was very large and resulted in extremely high pressure requirements to enable pumping of the fluids. The total volume of the small scale reactor was scaled up to enable the use of larger diameter tubing and the pumping of the fluids at an attainable pressure. The fluid flow calculations were determined based on: tubing ID, turbulent Reynolds's number, and time through each section of the reactor. See Table 3.1.

Initial Design Criteria

Target Volume (m^3)	Actual Volume (m^3)	Design N_{RE} in HXs
0.00004	0.000220	4000

Table 3.1

3.1.2 Turbulent Flow Requirement for Heat Transfer

The heat transfer calculations were constrained by the need to keep the flow in the tubing turbulent in order to maintain the most efficient heat transfer and enzyme reactions while minimizing the pressure drop across the total length of the tubing. For the design of the reactors, a Reynolds number of 4000 was selected as a design point. The lowest fully turbulent Reynolds number was selected because it was assumed that shear may affect the PCR reaction.

3.1.3 Temperature Ramp Rates

The temperature ramp rate design criteria was to have no less than 2.5 °C per second in temperature change. It was assumed that there is no maximum ramp rate.

4. Design of Heat Exchanger Test Device

Based on the above assumptions, a HETD was designed to have a total volume of 220 mL. The HETD consisted of a heat exchanger (HX1) to heat reaction buffer from 72 to 98 °C, a hold section (HOLD1) to hold the fluid temperature for 10 – 20 s and a second heat exchanger (HX2) to cool the fluids down again to 72°C. A bubble trap was used to eliminate bubbles from entering HX1 and flashing the fluids. See figure 4.1 for a schematic of the HETD. Table 4.1 contains the physical properties of water at the temperature set points of the three sections of the HETD.

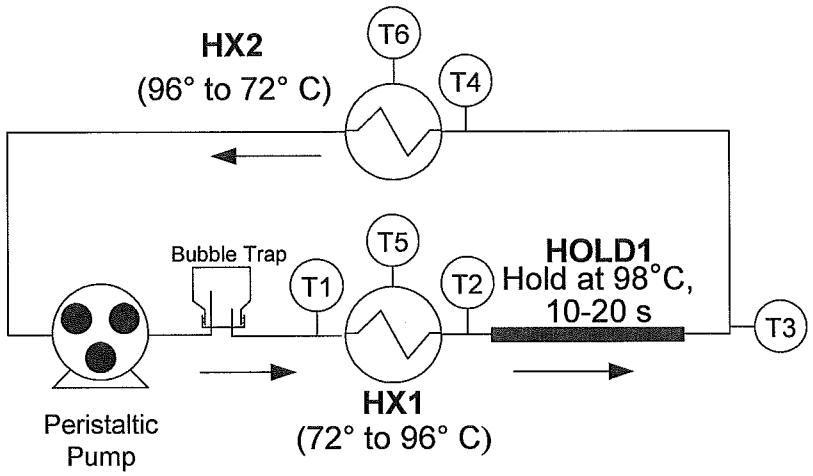

Figure 4.1

Fluid Flow and Heat Transfer Design Properties for Water

Section	Sect T (C)	Viscosity kg/(m*s)	Density (kg/m^3)	Specific Heat Cp (J/kgK)	k (W/m*K)
HX1	84.25	3.31E-04	968.0	4201	0.665
HOLD1	96.50	2.90E-04	962.0	4213	0.671
HX2	73.25	3.90E-04	975.9	4193	0.660

Table 4.1

4.1 Fluid Dynamic Calculations

The mass flow of the fluid heated per the above requirements was calculated based on the minimum temperature ramp rates and the hold time in HOLD1 of the fluid flowing through the reactor tubing. The calculation was further constrained by the need to keep the flow in the tubing turbulent for most efficient heat transfer and enzyme reactions while minimizing the pressure drop across the total length of the tubing.

Using the following equations, the data in tables 4.2 through 4.4 were obtained:

Mass Flow Rate

$$m_{dot} = \frac{1}{4}\pi ReD\mu \left[\frac{kg}{s}\right]$$

Where; D = inside tubing diameter [m]

$$\mu \left[\frac{kg}{m \cdot s}\right] = \text{viscosity}$$

$$Re = \frac{D\upsilon\rho}{\nu} = 4000[\ ]$$, turbulent conditions through heat exchangers

$$\rho \left[\frac{kg}{m^3}\right] = \text{density}$$

$$\upsilon = \text{linear velocity} \left[\frac{m}{s}\right]$$

Linear Velocity

$$\upsilon = \frac{m_{dot}}{\pi\rho r^2} \left[\frac{m}{s}\right]$$

$$r_i [m] = \text{inside tubing radius}$$

Ramp Rate

$$r_T \geq 2.5 \left[\frac{^oC}{s}\right]$$

Section Time

The section time is the time fluid has to flow through a section in order to match the ramp rate at the calculated linear velocity.

$T_{HX} = \frac{\Delta T_{HX}}{r_T}$ [s], the time the fluid has to change temperature at the ramp rate

$T_{HD} = 12$ [s], the time the fluid is held at the temperature exiting the heat exchanger

$\Delta T = 26$, the change in temperature across the heat exchangers $[^oC]$

Section Length

Heat Exchanger and Hold Lengths

The lengths were determined by utilizing the linear velocity and the section time.

$$L_{HX,HD} = \upsilon \cdot T_{HX,HD} \lfloor m \rfloor$$

Section Volume

$$V_{HX,HD} = \frac{\pi r^2}{L_{HX,HD}} \quad \lfloor m^3 \rfloor$$

4.1.1 Fluid Dynamic Calculations

HX1

ID (m)	Wall Thickness (m)	Mass Flow Rate (kg/s)	Velocity (m/s)	Ramp Rate (C/s)	Sect Time (s)	HX1 Length (m)	HX1 Vol (m^3)
0.003969	0.00119	0.0041	0.34	2.5	10.40	3.59	0.00004

Table 4.2

HOLD1

ID (m)	Wall Thickness (m)	Velocity (m/s)	Reynolds in HOLD (Re>4000?)	Sect Time (s)	HOLD1 Length (m)	HOLD1 Vol (m^3)
0.003969	0.00119	0.35	4570	12.00	4.16	0.00005

Table 4.3

HX2

ID (m)	Wall Thickness (m)	Mass Flow Rate (kg/s)	Velocity (m/s)	Ramp Rate (C/s)	HX2 Length (m)	HX2 Vol (m^3)
0.003969	0.00119	0.0041	0.34	4.1	2.18	0.000027

Table 4.4

The total calculated volume of the HETD was 123 mL, but with the additional peristaltic tubing the actual total volume of the reactor was 220 mL.

Friction Head Loss

The hydrodynamic pressure loss for the HETD loop was estimated as shown in table 4.5 below.

Le(length)=	32.6	ft
kinematic viscosity=	3.714E-06	ft^2/sec
ID=	0.0130	ft
flow area=	1.330E-04	ft^2
flow=	0.0002	cfs
velocity=	1.132	fps
NRe(Reynolds number)=	3968	
e(absolute roughness)=	1.5E-05	ft
e/D=	0.0012	
f(friction factor)=	0.0413	
Hf(total fictional head)=	2.1	ft
	0.9	**psig**

Table 4.5

4.2 Heat Exchanger Calculations

Once the fluid dynamic parameters and the lengths of the heat exchangers were calculated, the jacket temperature set points necessary to achieve the changes in temperature of the fluid were calculated utilizing the following algorithm. See Table 4.1, 4.6 and 4.7 for parameters used in calculating heat transfer properties.

Thermal Conductivity of HETD Materials of Construction

$k_{(PTFE)}$
0.25

Table 4.6

Jacket Side Individual Heat Transfer Coefficients

for Steam @10psig/115C
ho = 8517 W/m^2*K
for Water @ 15C
ho = 3000 W/m^2*K
for Air @90C
ho = 150 W/m^2*K

Table 4.7

Overall Energy Balance

The overall energy balance was calculated for use in determining the ΔT_{LMTD} once the overall heat transfer coefficient is known.

$$q = m_{dot}\, C_p \Delta T \left[W\right]$$ [1]

Where; $C_p\left[\frac{J}{kg \cdot K}\right]$ = specific heat of the fluid

[1] McCabe, W.L., Smith, J.C., Harriott, P. (1993) Unit Operations of Chemical Engineering. New York, NY: McGraw-Hill

ΔT [°C] = temperature difference between inlet and outlet of reactor sections

Heat Transfer by Forced Convection in Turbulent Flow

Overall Heat Transfer Coefficient

The overall heat transfer coefficient, U, was calculated for the heat exchange sections.

$$U = \frac{1}{h_i} + \frac{r_i}{r_o} \ln\left(\frac{r_o}{r_i}\right) + \frac{r_i}{h_o \cdot r_o} \left[\frac{W}{m^2 \cdot K}\right]$$

Where;

$h_i \left[\frac{W}{m^2 \cdot K}\right]$ = average individual heat transfer coefficient inside tube

$r_o [\mathrm{m}]$ = outside tubing radius

$h_o \left[\frac{W}{m^2 \cdot K}\right]$ = average individual heat transfer coefficient outside tube

The overall heat transfer coefficient for the separate reactor sections required the estimation of h_i, the individual heat transfer coefficient of the buffer used in the experimental tests. The individual heat transfer coefficient for the buffer was determined using the Nusselt number and the Dittus-Boelter equation for heat flow to a fluid in turbulent flow in a long straight pipe.

Dittus-Boelter equation

$$Nu = 0.023 \cdot \mathrm{Re}^{0.8} \cdot \mathrm{Pr}^{1/3} \cdot \phi^{0.14} \; [\,]$$

Where: $$\mathrm{Pr} = \frac{C_p \cdot \mu}{k} \; [\,]$$ Prandtl Number

$$\phi = \frac{\mu}{\mu_w} \; [\,]$$

μ = viscosity of the bulk fluid and

μ_w = viscosity of the fluid at the tube wall interface

The individual heat transfer coefficient was determined from the Nusselt number.

Nusselt number

$$h_i = \frac{Nu \cdot k}{D}$$

Once hi was determined, the overall heat transfer coefficient for each entire heat exchange section was calculated. The rate of heat transfer for each heat exchange section, q_T, equals the overall energy balance.

Overall Energy Balance

$$q_T = U \cdot A_T \cdot \Delta T_{LMTD} = q$$

The log mean temperature difference was solved for by rearranging the above equation.

Log Mean Temperature Difference

$$\Delta T_{LMTD} = \frac{q}{U \cdot A_T}$$

Where; $$A_T = \pi \cdot D \cdot L_{HX,HD} \; [m^2]$$ area of the heat transfer surface

Determination of Jacket Temperatures

The HETD heat exchangers were designed to have constant jacket temperatures for each section: T_{steam}, T_{air}, and T_{water} used in the shell side of each section. The equation for ΔT_{LMTD} when the jacket temperature is constant is calculated as follows.

$$\Delta T_{LMTD} = \frac{(T_s - T_2) - (T_s - T_1)}{\ln\left(\frac{T_s - T_2}{T_s - T_1}\right)}$$

The ΔT_{LMTD} was rearranged to solve for the jacket temperature.

$$T_s = \frac{T_2 - T_1 \cdot e^{\left(\frac{T_1 - T_2}{\Delta T_{LMTD}}\right)}}{1 - e^{\left(\frac{T_1 - T_2}{\Delta T_{LMTD}}\right)}}$$

$$T_1 = inlet\ temperature\ [^oC]$$

$$T_2 = outlet\ temperature\ [^oC]$$

$$T_s = jacket\ temperature\ [^oC]$$

HX1 72 to 98 in PTFE

q(W)	Pr	$\phi=\mu/\mu_w$	Nu	h_i (W/m^2*K)	U (W/m^2*K)	ΔT_{LMTD}	T_{steam}
451.1	2.1	1.1	25.8	4324	248	40.702	126.7

Table 4.8

HOLD1 @ 98 in PTFE

q(W)	Pr	$\phi=\mu/\mu_w$	Nu	h_i (W/m^2*K)	U (W/m^2*K)	ΔT_{LMTD}	T_{air}
14.6	1.8	1.0	24.2	4088	123	2.3	96.5

Table 4.9

HX2 (98 to 72) using water to cool in PTFE

q(W)	Pr	$\phi=\mu/\mu_w$	Nu	h_i (W/m^2*K)	U (W/m^2*K)	ΔT_{LMTD}	T_{water}
-451.1	2.1	1.1	25.8	4324	239.8	-69.3	15.0

Table 4.10

4.3 Construction of the HETD

The HETD was constructed of 5/32" ID PTFE tubing. The buffer was pumped through a small section of silicon tubing using a peristaltic pump. The PTFE tubing was insulated using larger diameter Pharmed tubing. See Figure 4.2 for construction photo.

4.3.1 Heat Exchanger (HX1)

Heat exchanger 1 (HX1) was constructed by passing 3.59 m of un-insulated PTFE tubing as calculated in Table 4.2 through a stainless steel steam vessel as in Figure 4.3. The shell side of HX1 was filled with saturated steam at 127

°C, T_{steam} , as calculated in Table 4.8. Thermocouples TC1 and TC2 were inserted in the inlet and outlet of HX1, respectively.

4.3.2 Hold Section

The hold section was coiled and insulated with large diameter Pharmed tubing and insulation batting. The inlet temperature was measured with TC2 and the outlet temperature was measured with TC3.

4.3.3 Heat Exchanger (HX2)

The HX2 heat exchanger had 2.18 m of tubing passed through chilled water at 15 °C, T_{water}, as calculated in Table 4.10.

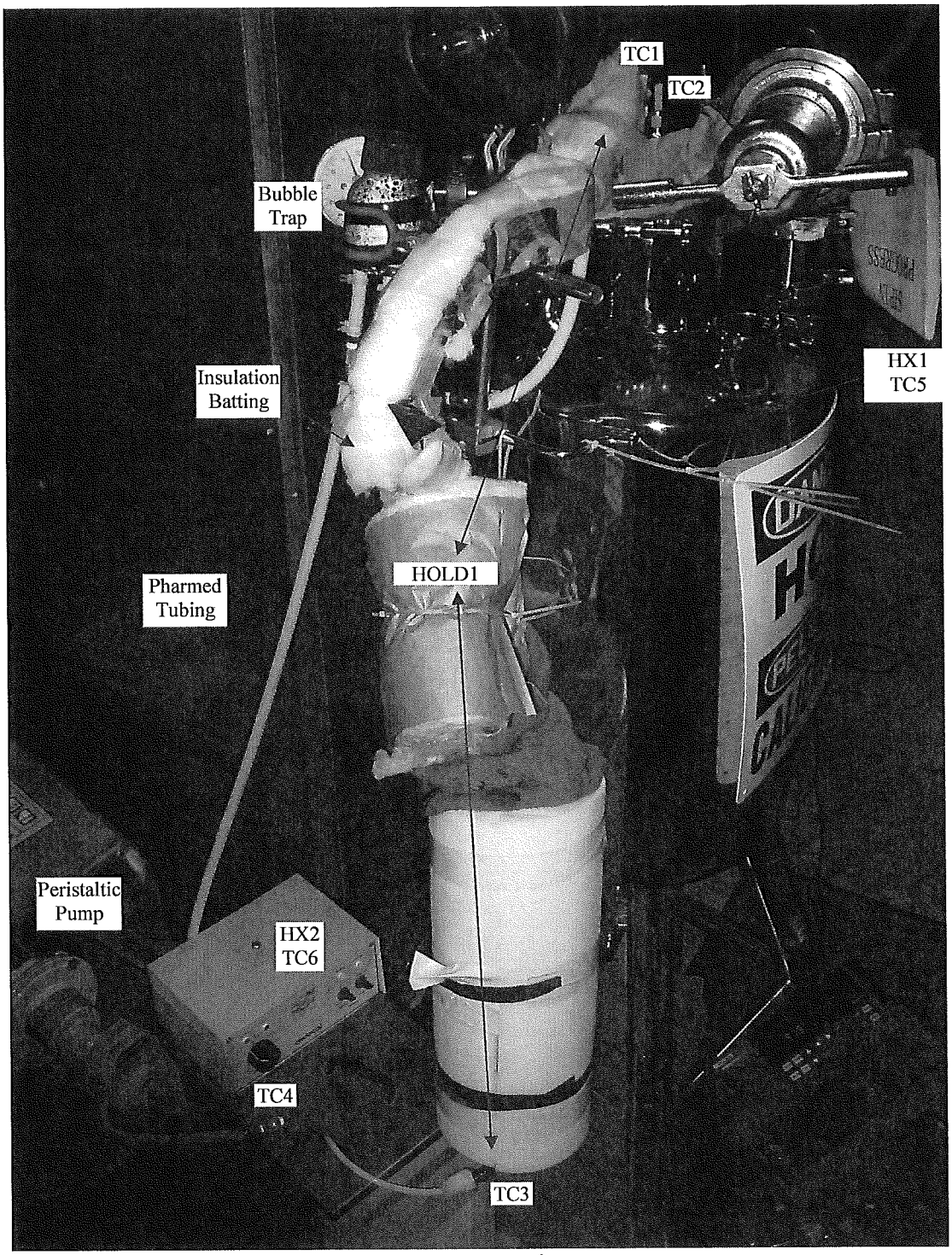
TC1
TC2
Bubble Trap
Insulation Batting
HX1 TC5
HOLD1
Pharmed Tubing
Peristaltic Pump
HX2 TC6
TC4
TC3

Figure 4.2

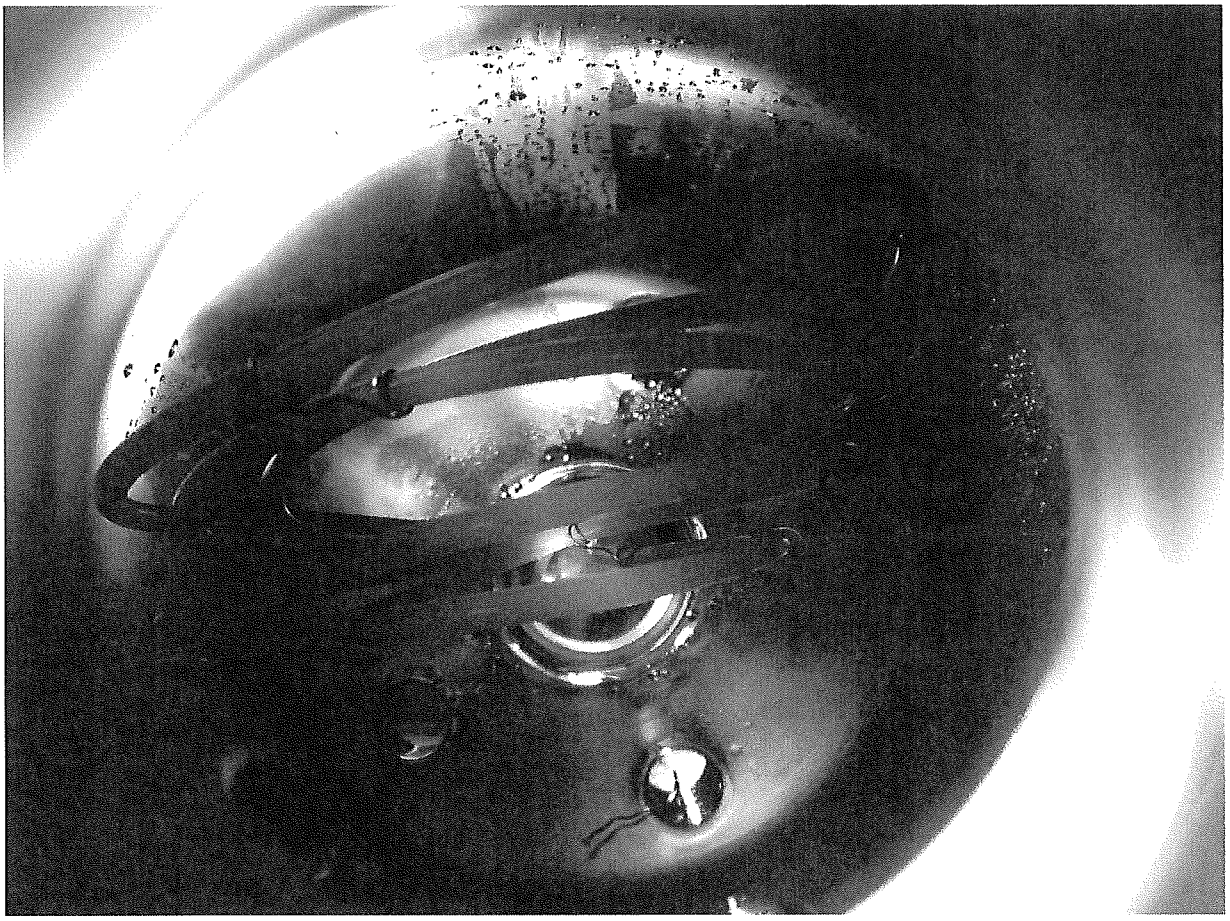

Figure 4.3

4.4 HETD Data Summary and Resultant Thermal Conductivity of Buffer

4.4.1 Temperature and Fluid Dynamic Data from Experimental Runs

Three separate experimental runs were made on the HETD. The averages of the data generated on the reactor are assembled in Tables 4.12 through 4.14.

Run Number	Date	Total Stable Run Time
1	16-May-06	0:50
2	17-May-06	1:55
3	17-May-06	1:07

Table 4.11

HX1 Fluid Dynamic Results

HX1	in HX1 Temp 1	out HX1 Temp 2	Steam Temp 5	Avg Temp	HX1 ΔT	ΔT_{LMTD}	Viscosity kg/(m*s)	Density (kg/m^3)	Specific Heat Cp (J/kgK)	k(water) (W/m*K)	Velocity (m/s)	Mass Flow Rate (kg/s)
Run	C	C	C	C	C	C	kg/(m*s)	(kg/m^3)	(J/kgK)	(W/m*K)	(m/s)	(kg/s)
1	71.4	96.5	126.0	84.0	25.1	40.7	3.3E-04	969.4	4200.7	0.7	0.3	4.11E-03
2	72.2	97.0	126.0	84.6	24.8	40.2	3.3E-04	968.2	4201.2	0.7	0.3	4.13E-03
3	71.0	96.9	125.9	83.9	25.9	40.6	3.3E-04	968.3	4200.6	0.7	0.3	4.09E-03
Overall Average	71.5	96.8	126.0	84.2	25.3	40.5	3.32E-04	968.6	4201	0.665	0.34	4.11E-03

Table 4.12

HOLD1 Fluid Dynamic Results

HOLD1	out HX1 Temp 2	out HOLD1 Temp 3	Hold Temp (C)	Avg Temp	HOLD1 ΔT	ΔT_{LMTD}	Viscosity kg/(m*s)	Density (kg/m^3)	Specific Heat Cp (J/kgK)	k(water) (W/m*K)	Velocity (m/s)	Mass Flow Rate (kg/s)
Run	C	C	C	C	C	C	kg/(m*s)	(kg/m^3)	(J/kgK)	(W/m*K)	(m/s)	(kg/s)
1	96.5	96.2	90.0	96.4	-0.3	-6.4	2.9E-04	964.5	4212.5	0.7	0.3	4.09E-03
2	97.0	96.8	90.0	96.9	-0.2	-6.9	2.9E-04	960.0	4213.0	0.7	0.3	4.09E-03
3	96.9	96.6	95.6	96.7	-0.3	-1.2	2.9E-04	962.8	4212.9	0.7	0.3	4.07E-03
Overall Average	96.8	96.5	91.9	96.7	-0.3	-4.8	2.90E-04	962.4	4213	0.671	0.34	4.08E-03

Table 4.13

HX2 Fluid Dynamic Results

HX2	in HX2 Temp 3	out HX2 Temp 4	Chiller Temp 6	Avg Temp	HX2 ΔT	ΔT_{LMTD}	Viscosity kg/(m*s)	Density (kg/m^3)	Specific Heat Cp (J/kgK)	k(water) (W/m*K)	Velocity (m/s)	Mass Flow Rate (kg/s)
Run	C	C	C	C	C	C	Kg/(m*s)	(kg/m^3)	(J/kgK)	(W/m*K)	(m/s)	(kg/s)
1	96.2	73.9	17.0	85.1	-22.3	-67.4	3.3E-04	968.4	4201.6	0.7	0.3	4.17E-03
2	96.8	74.8	16.6	85.8	-22.0	-68.5	3.2E-04	967.1	4202.2	0.7	0.4	4.19E-03
3	96.6	73.5	17.0	85.0	-23.1	-67.3	3.3E-04	968.1	4201.6	0.7	0.3	4.16E-03
Overall Average	96.5	74.1	16.9	85.3	-22.5	-67.8	3.27E-04	967.9	4202	0.666	0.35	4.17E-03

Table 4.14

4.4.2 HETD Heat Transfer Data Calculated from Experimental Runs

Using the design calculations for the heat exchange sections, h_i and h_o were calculated at the average temperature of each section. See Tables 4.15 through 4.17 for the data summary.

HX1 Heat Exchanger Calculation Results

HX1	q = mCpΔT	U = q/(A*ΔTlmtd)	Re = vDρ/μ	Pr = Cpμ/k	$\phi=\mu/\mu_w$	Nu = $0.023*Re^{.8}Pr^{(1/3)}\phi^{.14}$	h_i (W/m^2*K)	ho = ((Ro/Ri)*(1/U-1/hi-(Ri/k*LN(Ro/Ri))^-1
Run	(W)	(W/m^2*K)	[]	[]	[]	[]	(W/m^2*K)	(W/m^2*K)
1	433.4	238.1	4581.6	1.8	1.2	27.5	4605.4	2678.3
2	429.2	238.7	4598.2	1.8	1.1	27.5	4615.0	2567.9
3	445.3	245.0	4562.7	1.8	1.2	27.4	4590.6	7083.5
Overall Average	435.95	240.6	4581	1.8	1.2	27.5	4604	4110

Table 4.15

HOLD1 Heat Exchanger Calculation Results

HOLD1	q = mCpΔT	U = q/(A*ΔTlmtd)	Re = vDρ/μ	Pr = Cpμ/k	$\phi=\mu/\mu_w$	Nu = $0.023*Re^{.8}Pr^{(1/3)}\phi^{.14}$	h_i (W/m^2*K)	ho = ((Ro/Ri)*(1/U-1/hi-(Ri/k*LN(Ro/Ri))^-1
Run	(W)	(W/m^2*K)	[]	[]	[]	[]	(W/m^2*K)	(W/m^2*K)
1	-5.8	17.6	4511.1	1.8	1.0	26.6	4503.8	12.2
2	-3.1	10.1	4511.9	1.8	1.0	26.6	4503.9	7.3
3	-5.5	100.5	4489.4	1.8	1.0	26.5	4486.0	150.2
Overall Average	-4.79	42.7	4504	1.8	1.0	26.6	4498	57

Table 4.16

HX2 Heat Exchanger Calculation Results

HX2	q = mCpΔT	U = q/(A*ΔTlmtd)	Re = vDρ/μ	Pr = Cpμ/k	$\phi=\mu/\mu_w$	Nu = $0.023*Re^{.8}Pr^{(1/3)}\phi^{.14}$	h_i (W/m^2*K)	ho = ((Ro/Ri)*(1/U-1/hi-(Ri/k*LN(Ro/Ri))^-1
Run	(W)	(W/m^2*K)	[]	[]	[]	[]	(W/m^2*K)	(W/m^2*K)
1	-390.4	129.5	4088.3	2.1	1.0	25.7	4304.0	166.5
2	-387.7	126.5	4143.3	2.0	1.0	25.9	4338.3	158.6
3	-403.4	134.0	4071.6	2.1	1.0	25.6	4291.0	178.7
Overall Average	-393.83	130.0	4101	2.1	1.0	25.7	4311	168

Table 4.17

5. Design of a Large Scale PCR Reactor

Based on the results from the HETD tests, the physical property assumptions and the thermal restriction of PCR fluids, a large scale reactor was designed to have a total volume of 305 mL. The large scale reactor consisted of; a denaturing heat exchanger (HX1) to heat reaction mix from 72 to 98 °C, a hold section (HOLD1) to hold the fluid temperature for 10 – 20 s, an annealing heat exchanger (HX2) to cool the fluids down to 50°C with a hold section (HOLD2) to hold the reaction mix temperature for 10 – 20 s, and an elongation heat exchanger (HX3) to heat the reaction mix to 72°C with a 60 to 120 s hold section (HOLD3). A bubble trap was used to eliminate bubbles from entering HX1 and flashing the fluids. Table 5.1 contains the physical properties of water at the temperature set points of the six sections of the large scale reactor.

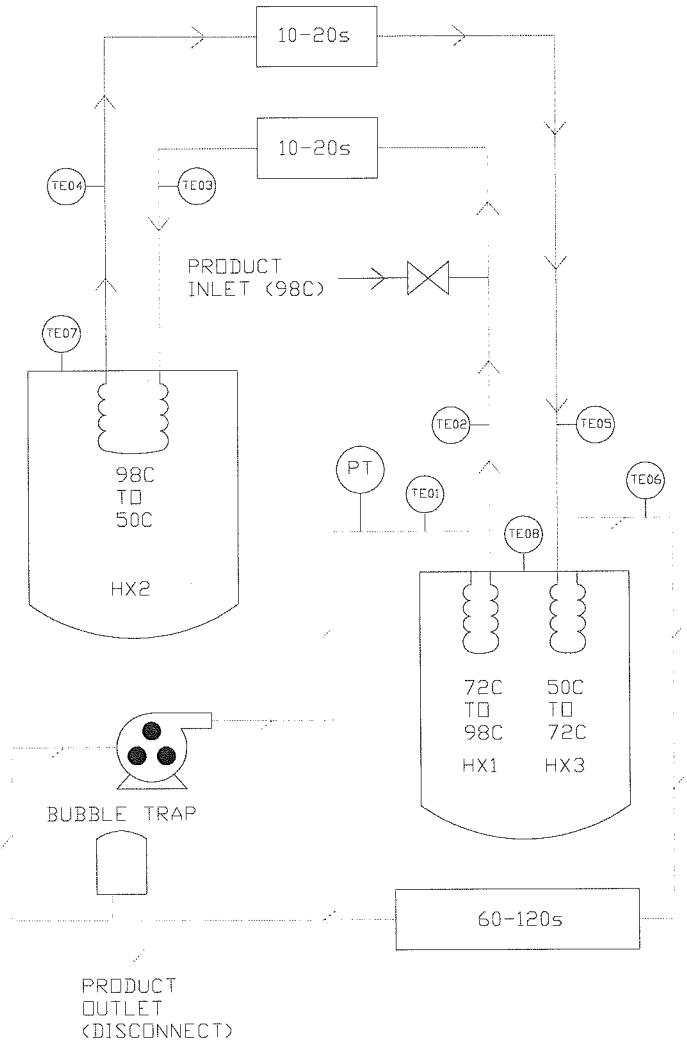

Figure 5.1

PCR Reactor Fluid Physical Properties for Design

Section	Sect T (C)	Viscosity kg/(m*s)	Density (kg/m^3)	Specific Heat Cp (J/kgK)	k(RxnMx) (W/m*K)
HX1	85	3.28E-04	967	4202	0.666
HOLD1	98	2.88E-04	962	4214	0.672
HX2	74	3.85E-04	975	4193	0.660
HOLD2	50	5.49E-04	989	4181	0.648
HX3	61	4.66E-04	980	4186	0.654
HOLD3	72	3.97E-04	977	4192	0.659

Table 5.1

5.1 Fluid Dynamic Calculations

The fluid dynamic design calculations for the reactor used the same design algorithm used on the HETD. It was assumed that the Reynolds number in HOLD2 would be the limiting design criteria due to being the lowest temperature section. Therefore, a Reynolds Number of 2300 in HOLD2 was used a design start point. See table 5.2 and 5.3 for the design summaries.

Resultant Reynolds Numbers in Heat Exchangers

Reynolds in HX1	Reynolds in HX2	Reynolds in HX3
8759	7453	6155

Table 5.2

Large Scale Reactor Design Calulation Totals

Total Head (psig)	13.7
Total Volume Holdup (mL)	305.4
Total HX Length (ft)	4.61
Total Hold Length (ft)	92.00
Cycle Time (s)	95
30 Cycle Time (min)	47

Table 5.3

5.2 Heat Exchanger Calculations

Once the fluid dynamic parameters and the lengths of each reactor section were calculated, the jacket temperature set points necessary to achieve the changes in temperature of the fluid in each section were calculated utilizing the HETD design algorithm. The reactor heat exchangers used 316L stainless steel to enable rapid heat transfer and the hold sections were designed to be constructed of PTFE to better insulate the reaction fluids. HX1 and HX3 were designed to use the same heat exchanger. See Table 5.1, 5.11, 5.12 for parameters used in calculating heat transfer properties.

Thermal Conductivity of Large Scale Reactor Materials of Construction

$k_{(PTFE)}$	$k_{(316L)}$
0.25	17

Table 5.11
Jacket Side Individual Heat Transfer Coefficients

Jacket Side Properties for Steam @10psig/115C
ho = 8517 W/m^2*K
Jacket Water
ho = 2142 W/m^2*K

Table 5.12

5.3 Construction of the PCR Reactor

The reactor was constructed of 1/16" ID 316L SS tubing, 1/8" ID PTFE tubing and 5/32" ID PTFE tubing. The buffer was pumped through a small section of silicon tubing using a dual head peristaltic pump. The PTFE tubing was insulated using larger diameter Pharmed tubing and insulating spray foam. See Figure 5.2 for construction photo.

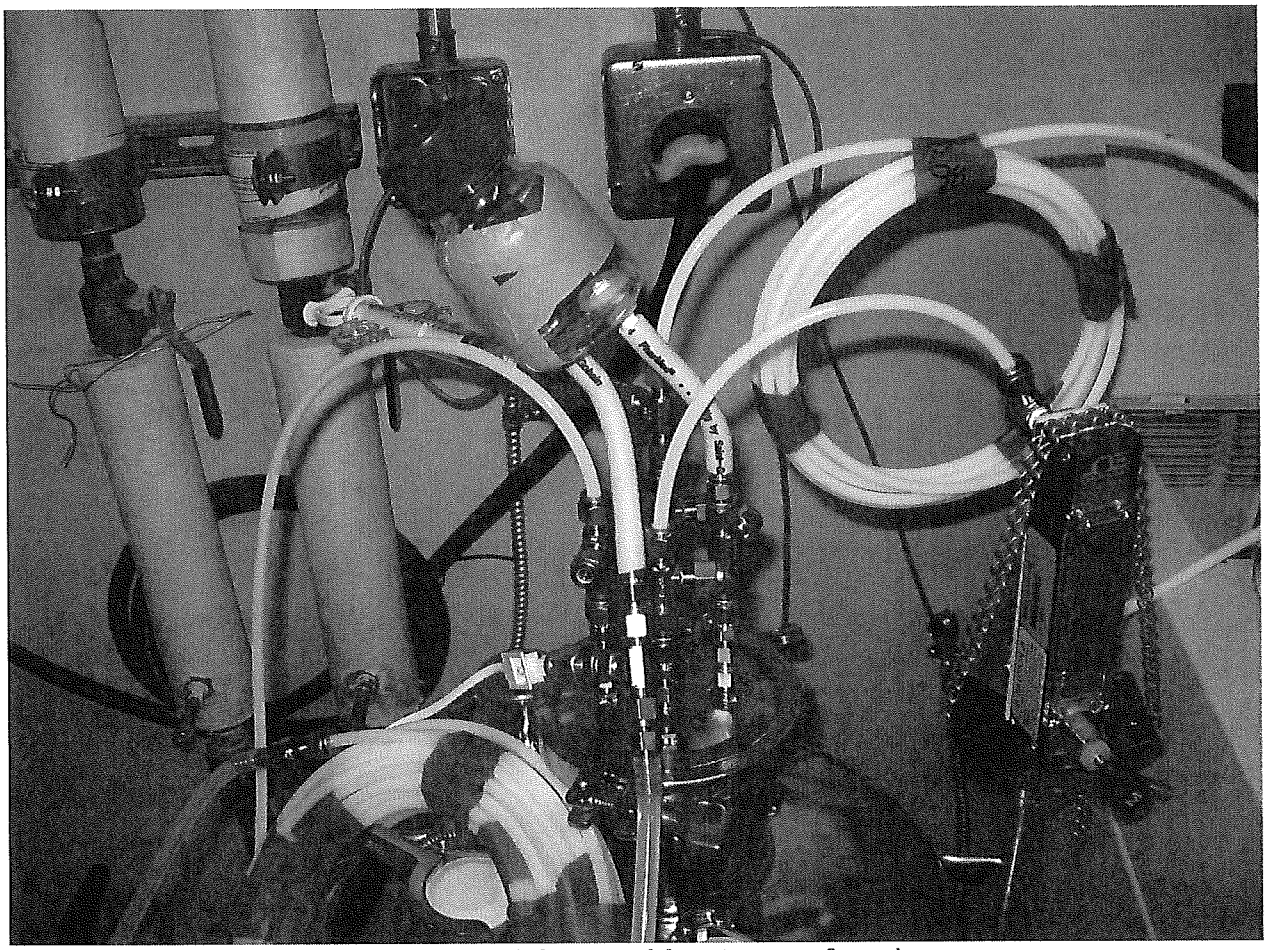

Figure 5.2(shown without spray foam)

5.3.1 Heat Exchanger (HX1)

Heat exchanger 1 (HX1) was constructed by passing 0.508m of un-insulated 316L SS tubing as empirically determined from repeated testing. This varies slightly from the design as the actual steam temperature was lower. The shell side of HX1 was filled with saturated steam at 108 °C, T_{steam}. Thermocouple temperature elements (TE)1 and TE 2 were inserted in the inlet and outlet of HX1, respectively.

5.3.2 Hold Section 1

The hold section was coiled and insulated with large diameter Pharmed tubing and spray foam insulation. The inlet temperature was measured with TE2 and the outlet temperature was measured with TE3.

5.3.3 Heat Exchanger (HX2)

The HX2 heat exchanger had 0.762 m of 316L tubing passed through chilled water at 13 °C, T_{water}.

5.3.4 Hold Section 2

The hold section was coiled and insulated with large diameter Pharmed tubing and spray foam insulation. The inlet temperature was measured with TE4 and the outlet temperature was measured with TE5

5.3.5 Heat Exchanger (HX3)

Heat exchanger 3 (HX3) was constructed by passing 0.254 m of un-insulated 316L SS tubing as empirically determined from repeated testing. This varies slightly from the design as the steam temperature actual was lower. The shell side of HX3 was filled with saturated steam at 108 °C, T_{steam}. Thermocouples TE 5 and TE 6 were inserted in the inlet and outlet of HX3, respectively.

5.3.6 Hold Section 3

The hold section was coiled and insulated with large diameter Pharmed tubing and spray foam insulation. The inlet temperature was measured with TE6 and the outlet temperature was measured with TE1.

5.3.7 System Components

Temperature Elements

The temperature elements are standard thermocouples. They have been sealed in Teflon tubing to allow direct contact with the flow. TE placement is before and after the holds, with TE 7 detecting chilled water temperature and TE 8 detecting steam temperature.

Pump and Pressure Transmitter

The pump is a dual peristaltic. The pressure transmitter connects to the pump, and is adapted to the product flow using lure and swagelock fittings. Flow is determined using a flow meter.

Bubble Trap

The bubble trap is constructed using a standard 125 ml plastic container. The holdup in the bubble trap is approximately 10-20 ml.

Product Inlet

The product inlet is designed for a hot start, injecting the master mix at 96 °C. It consists of a lure fitting for a syringe, and the necessary adapters.

5.3.8 Start-Up Tests

Several experiments were needed before testing actual product. These are hydrodynamic testing, dye testing, water runs and finally buffer runs.

Hydrodynamic Testing

Once all the connections were made, the system was tested for leaks. This was done using both an open and closed loop, with DI water as the solution. There were several small leaks, which were fixed by tightening or re-orienting fittings. Once the system was virtually leak-proof, it was ready for further testing.

Dye Testing

Although the total cycle and hold times were calculated, a dye test was conducted to ensure accuracy. This was accomplished by starting the system

in a closed loop, using DI water. A dyed sample of DI water, which was approximately the same volume as the master mix to be injected during a product run, was injected so the dye could be observed as it flowed through the system.
The following results were recorded:

Hold step one: 13 seconds
Hold step two: 10 seconds
Hold step three: 76 seconds
Total cycle time: 131 seconds

All of these times fell within acceptable parameters. It was also observed that the system kept relatively stable slug flow throughout a cycle. Since the system is turbulent, this is expected to decay over time.

Water Runs
A series of water runs were conducted to ensure the temperature setpoints stayed within established parameters, and to determine if any adjustments to the heat exchanger coil lengths needed to be made. After the first water run, it was apparent that the HX2 coil length was not long enough. Instead of adjusting the flow, which would affect the hold times, the length was eventually extended. This allowed the system to reach the desired setpoint. Once that setpoint was reached, the 50°C to 72°C heat exchange was determined to require more coil length. This was also extended. With this change, all setpoints were within established parameters. Since previous experiments showed little change when using buffer solution, this setup was used for the buffer runs.

Buffer Runs
Using established parameters and setup, three separate buffer runs were conducted to ensure stability during a product run. Each run has all temperature elements recorded. Through analyzing the data, it is determined that once all set points are achieved, the system remains stable and within all parameters.
The following three graphs, Figures 5.3, 5.4 and 5.5, show the temperature data for each buffer run. The yellow section indicates that all the set points have been reached.

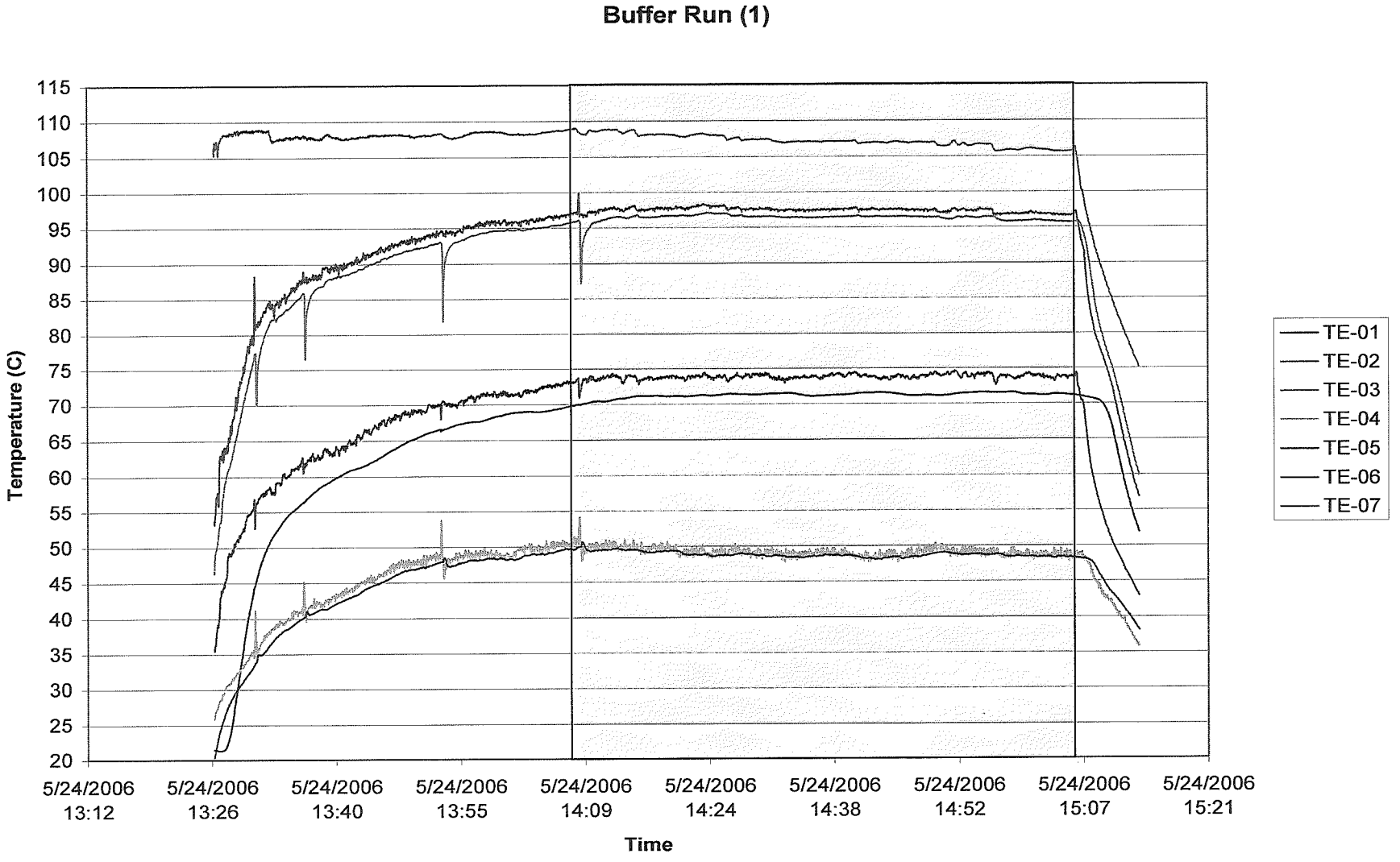
Buffer Run (1)
Temperature (C)
115
110
105
100
95
90
85
80
75
70
65
60
55
50
45
40
35
30
25
20
5/24/2006 13:12
5/24/2006 13:26
5/24/2006 13:40
5/24/2006 13:55
5/24/2006 14:09
5/24/2006 14:24
5/24/2006 14:38
5/24/2006 14:52
5/24/2006 15:07
5/24/2006 15:21
Time
TE-01
TE-02
TE-03
TE-04
TE-05
TE-06
TE-07

Figure 5.3

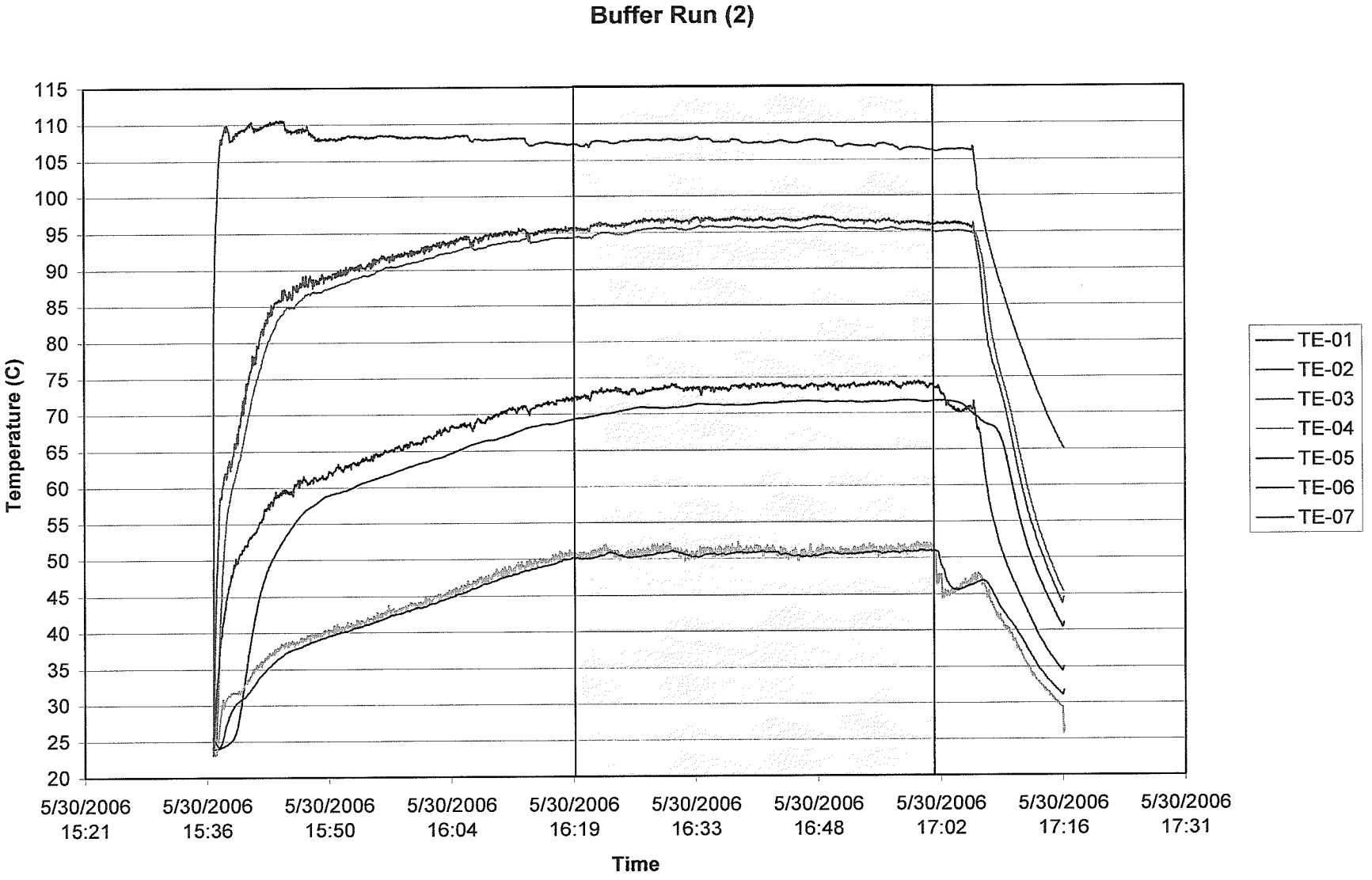
Buffer Run (2)
Temperature (C)
115
110
105
100
95
90
85
80
75
70
65
60
55
50
45
40
35
30
25
20
5/30/2006 15:21
5/30/2006 15:36
5/30/2006 15:50
5/30/2006 16:04
5/30/2006 16:19
5/30/2006 16:33
5/30/2006 16:48
5/30/2006 17:02
5/30/2006 17:16
5/30/2006 17:31
Time
TE-01
TE-02
TE-03
TE-04
TE-05
TE-06
TE-07

Figure 5.4

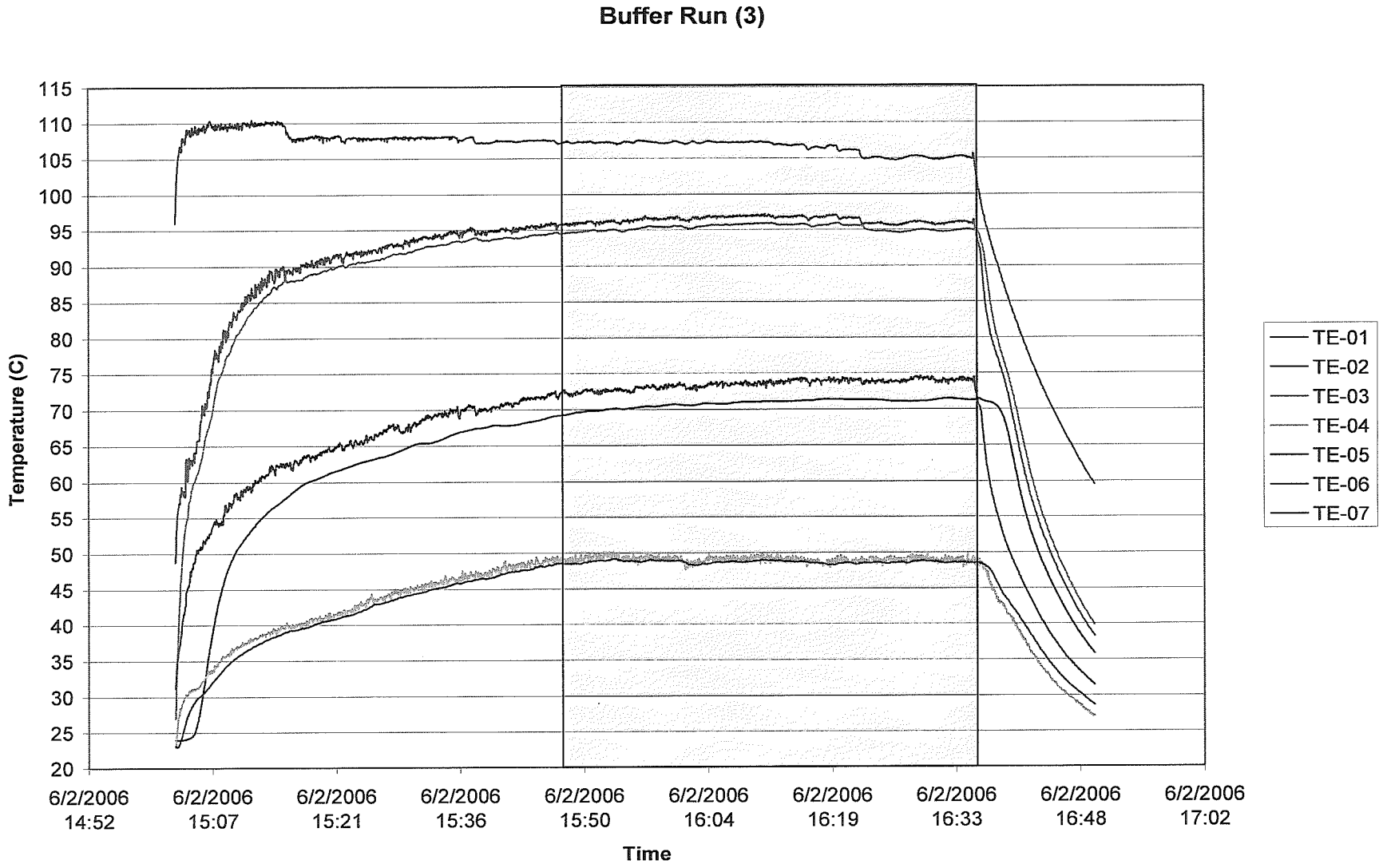
Buffer Run (3)
Temperature (C)
115
110
105
100
95
90
85
80
75
70
65
60
55
50
45
40
35
30
25
20
6/2/2006 14:52
6/2/2006 15:07
6/2/2006 15:21
6/2/2006 15:36
6/2/2006 15:50
6/2/2006 16:04
6/2/2006 16:19
6/2/2006 16:33
6/2/2006 16:48
6/2/2006 17:02
Time
TE-01
TE-02
TE-03
TE-04
TE-05
TE-06
TE-07

Figure 5.5

5.4 PCR Reactor Data Summary and Resultant Thermal Conductivity of Buffer

5.4.1 Temperature and Fluid Dynamic Data from Experimental Runs

Three separate experimental runs with Buffer were made on the large scale reactor. The averages of the data generated on the large scale reactor are assembled in Tables 5.19 through 5.25.

Run Number	Date	Total Stable Run Time
1	24-May-06	1:16
2	30-May-06	0:50
3	2-Jun-06	0:53

Table 5.19

HX1 Fluid Dynamic Results

HX1	in HX1 TC 1	out HX1 TC 2	Steam TC 7	Avg Temp	HX1 ΔT	ΔT_{LMTD}	Viscosity	Density	Specific Heat Cp	k(water)	Velocity	Mass Flow Rate
Run	°C	°C	°C	°C	°C	°C	kg/(m*s)	(kg/m^3)	(J/kgK)	(W/m*K)	(m/s)	(kg/s)
1	70.5	96.9	107.4	83.7	26.4	20.9	2.973E-04	972.9	4225.1	0.7	1.9	2.81E-03
2	70.7	96.3	107.3	83.5	25.6	21.3	3.348E-04	969.5	4200.3	0.7	1.9	2.80E-03
3	70.6	96.2	106.5	83.4	25.6	20.5	3.351E-04	969.5	4200.2	0.7	1.9	2.80E-03
Overall Average	70.6	96.5	107.1	83.5	25.9	20.9	3.22E-04	970.6	4209	0.669	1.88	2.80E-03

Table 5.20

HOLD1 Fluid Dynamic Results

HOLD1	out HX1 TC 2	in HX2 TC 3	Hold Temp	Avg Temp	HX1 ΔT	ΔT_{LMTD}	Viscosity	Density	Specific Heat Cp	k(water)	Velocity	Mass Flow Rate
Run	°C	°C	°C	°C	°C	°C	kg/(m*s)	(kg/m^3)	(J/kgK)	(W/m*K)	(m/s)	(kg/s)
1	96.9	95.8	90.0	96.4	-1.1	-6.4	2.904E-04	960.0	4212.5	0.7	0.4	2.77E-03
2	96.3	95.2	90.0	95.7	-1.1	-5.7	2.914E-04	961.7	4211.8	0.7	0.4	2.77E-03
3	96.2	95.1	90.0	95.7	-1.1	-5.7	2.915E-04	961.7	4211.8	0.7	0.4	2.77E-03
Overall Average	96.5	95.4	90.0	95.9	-1.1	-5.9	2.91E-04	961.2	4212	0.671	0.36	2.77E-03

Table 5.21

HX2 Fluid Dynamic Results

HX2	in HX2 TC 3	out HX2 TC 4	Chiller TC 8	Avg Temp	HX1 ΔT	ΔT_{LMTD}	Viscosity	Density	Specific Heat Cp	k(water)	Velocity	Mass Flow Rate
Run	°C	°C	°C	°C	°C	°C	kg/(m*s)	(kg/m^3)	(J/kgK)	(W/m*K)	(m/s)	(kg/s)
1	95.8	49.1	14.2	72.5	-46.6	-55.1	3.942E-04	977.9	4192.0	0.7	1.9	2.82E-03
2	95.2	50.8	9.8	73.0	-44.4	-60.5	3.911E-04	977.3	4192.3	0.7	1.9	2.82E-03
3	95.2	49.0	16.3	72.1	-46.2	-52.5	3.964E-04	977.8	4191.7	0.7	1.9	2.82E-03
Overall Average	95.4	49.6	13.4	72.5	-45.7	-56.0	3.94E-04	977.6	4192	0.659	1.88	2.82E-03

Table 5.22

HOLD2 Fluid Dynamic Results

HOLD2	out HX2 TC 4	in HX3 TC 5	Hold Temp	Avg Temp	HX1 ΔT	ΔT_{LMTD}	Viscosity	Density	Specific Heat Cp	k(water)	Velocity	Mass Flow Rate
Run	°C	°C	°C	°C	°C	°C	kg/(m*s)	(kg/m^3)	(J/kgK)	(W/m*K)	(m/s)	(kg/s)
1	49.1	48.7	46.0	48.9	-0.5	-2.9	5.587E-04	994.7	4181.2	0.6	0.4	2.87E-03
2	50.8	50.3	46.0	50.6	-0.5	-4.6	5.445E-04	991.6	4181.6	0.6	0.4	2.86E-03
3	49.0	48.6	46.0	48.8	-0.4	-2.8	5.598E-04	992.5	4181.1	0.6	0.4	2.86E-03
Overall Average	49.6	49.2	46.0	49.4	-0.4	-3.4	5.54E-04	992.9	4181	0.648	0.36	2.86E-03

Table 5.23

HX3 Fluid Dynamic Results

HX3	in HX3 TC 5	out HX3 TC 6	Steam TC 7	Avg Temp	HX1 ΔT	ΔT_{LMTD}	Viscosity	Density	Specific Heat Cp	k(water)	Velocity	Mass Flow Rate
Run	°C	°C	°C	°C	°C	°C	kg/(m*s)	(kg/m^3)	(J/kgK)	(W/m*K)	(m/s)	(kg/s)
1	48.7	73.2	107.4	60.9	24.5	45.3	4.669E-04	985.4	4185.5	0.7	1.9	2.84E-03
2	50.3	73.2	107.3	61.8	22.9	44.6	4.612E-04	983.0	4185.9	0.7	1.9	2.83E-03
3	48.6	73.3	106.5	60.9	24.7	44.4	4.669E-04	984.0	4185.5	0.7	1.9	2.84E-03
Overall Average	49.2	73.2	107.1	61.2	24.0	44.8	4.65E-04	984.1	4186	0.654	1.88	2.84E-03

Table 5.24

HOLD3 Fluid Dynamic Results

HOLD3	out HX3 TC 6	in HX1 TC 1	Hold Temp	Avg Temp	HX1 ΔT	ΔT_{LMTD}	Viscosity	Density	Specific Heat Cp	k(water)	Velocity	Mass Flow Rate
Run	°C	°C	°C	°C	°C	°C	kg/(m*s)	(kg/m^3)	(J/kgK)	(W/m*K)	(m/s)	(kg/s)
1	73.2	70.5	60.0	71.9	-2.7	-11.8	3.978E-04	978.1	4191.6	0.7	0.2	2.82E-03
2	73.2	70.7	60.0	72.0	-2.5	-11.9	3.971E-04	977.7	4191.7	0.7	0.2	2.82E-03
3	73.2	70.5	60.0	71.9	-2.7	-11.8	3.976E-04	977.7	4191.6	0.7	0.2	2.82E-03
Overall Average	73.2	70.6	60.0	71.9	-2.6	-11.9	3.97E-04	977.8	4192	0.659	0.23	2.82E-03

Table 5.25

5.4.2 PCR Reactor Heat Transfer Data Calculated from Experimental Runs

Using the design calculations for the heat exchange sections, hi and ho were calculated at the average temperature of each section. See Tables 5.26 through 5.31 for the data summary.

HX1 Heat Exchanger Calculation Results

HX1	q = mCpΔT	U = q/(A*ΔTlmtd)	Re = vDρ/μ	Pr = Cpμ/k	$\phi=\mu/\mu_w$	Nu = $0.023*Re^{.8}Pr^{(1/3)}\phi^{.14}$	h_i (W/m^2*K)	ho = ((Ro/Ri)*(1/U-1/hi-(Ri/k*LN(Ro/Ri))^-1
Run	(W)	(W/m^2*K)	[]	[]	[]	[]	(W/m^2*K)	(W/m^2*K)
1	313.3	6735.3	7661.0	2.1	0.9	41.8	20271.4	6775.0
2	300.0	6310.1	7610.1	2.1	1.0	42.5	20232.6	5847.8
3	300.9	6613.7	7602.5	2.1	1.0	42.5	20222.3	6491.1
Overall Average	304.73	6553.0	7625	2.1	1.0	42.3	20242	6371

Table 5.26

HOLD1 Heat Exchanger Calculation Results

HOLD1	q = mCpΔT	U = q/(A*ΔTlmtd)	Re = vDρ/μ	Pr = Cpμ/k	$\phi=\mu/\mu_w$	Nu = $0.023*Re^{.8}Pr^{(1/3)}\phi^{.14}$	h_i (W/m^2*K)	ho = ((Ro/Ri)*(1/U-1/hi-(Ri/k*LN(Ro/Ri))^-1
Run	(W)	(W/m^2*K)	[]	[]	[]	[]	(W/m^2*K)	(W/m^2*K)
1	-13.4	47.2	3825.2	1.8	1.0	23.3	4932.6	21.2
2	-12.6	45.0	3817.0	1.8	1.0	23.3	4928.4	28.9
3	-12.8	45.5	3815.6	1.8	1.0	23.3	4927.3	29.4
Overall Average	-12.92	45.9	3819	1.8	1.0	23.3	4929	27

Table 5.27

HX2 Heat Exchanger Calculation Results

HX2	q = mCpΔT	U = q/(A*ΔTlmtd)	Re = vDρ/μ	Pr = Cpμ/k	$\phi=\mu/\mu_w$	Nu = $0.023*Re^{.8}Pr^{(1/3)}\phi^{.14}$	h_i (W/m^2*K)	ho = ((Ro/Ri)*(1/U-1/hi-(Ri/k*LN(Ro/Ri))^-1
Run	(W)	(W/m^2*K)	[]	[]	[]	[]	(W/m^2*K)	(W/m^2*K)
1	-551.2	2993.6	6519.2	2.5	1.0	39.7	18760.3	1781.6
2	-524.4	2613.9	6567.5	2.5	1.0	39.9	18826.8	1492.4
3	-545.8	3112.9	6481.8	2.5	1.0	39.6	18705.5	1880.4
Overall Average	-540.45	2906.8	6523	2.5	1.0	39.8	18764	1718

Table 5.28

HOLD2 Heat Exchanger Calculation Results

HOLD2	q = mCpΔT	U = q/(A*ΔTlmtd)	Re = vDρ/μ	Pr = Cpμ/k	$\phi=\mu/\mu_w$	Nu = $0.023*Re^{.8}Pr^{(1/3)}\phi^{.14}$	h_i (W/m^2*K)	ho = ((Ro/Ri)*(1/U-1/hi-(Ri/k*LN(Ro/Ri))^-1
Run	(W)	(W/m^2*K)	[]	[]	[]	[]	(W/m^2*K)	(W/m^2*K)
1	-5.7	39.0	2058.7	3.6	1.0	17.8	3640.1	29.5
2	-5.5	26.0	2105.9	3.5	1.0	18.0	3678.2	17.7
3	-4.6	33.8	2050.0	3.6	1.0	17.8	3630.0	25.1
Overall Average	-5.26	33.0	2072	3.6	1.0	17.9	3649	24

Table 5.29

HX3 Heat Exchanger Calculation Results

HX3	q = mCpΔT	U = q/(A*ΔTlmtd)	Re = vDρ/μ	Pr = Cpμ/k	$\phi=\mu/\mu_w$	Nu = $0.023*Re^{.8}Pr^{(1/3)}\phi^{.14}$	h_i (W/m^2*K)	ho = ((Ro/Ri)*(1/U-1/hi-(Ri/k*LN(Ro/Ri))^-1
Run	(W)	(W/m^2*K)	[]	[]	[]	[]	(W/m^2*K)	(W/m^2*K)
1	291.9	5792.7	5546.9	3.0	1.0	37.0	17332.3	5482.3
2	271.4	5466.5	5601.3	3.0	1.0	37.2	17405.2	4809.8
3	293.2	5932.7	5537.6	3.0	1.0	37.0	17310.0	5761.9
Overall Average	285.52	5730.6	5562	3.0	1.0	37.1	17349	5351

Table 5.30

HOLD3 Heat Exchanger Calculation Results

HOLD3	q = mCpΔT	U = q/(A*ΔTlmtd)	Re = vDρ/μ	Pr = Cpμ/k	$\phi=\mu/\mu_w$	Nu = $0.023*Re^{.8}Pr^{(1/3)}\phi^{.14}$	h_i (W/m^2*K)	ho = ((Ro/Ri)*(1/U-1/hi-(Ri/k*LN(Ro/Ri))^-1
Run	(W)	(W/m^2*K)	[]	[]	[]	[]	(W/m^2*K)	(W/m^2*K)
1	-32.0	12.2	2274.6	2.5	1.0	17.2	2851.5	8.1
2	-29.5	11.1	2277.4	2.5	1.0	17.2	2853.0	7.3
3	-31.9	11.9	2274.8	2.5	1.0	17.2	2851.3	7.8
Overall Average	-31.13	11.7	2276	2.5	1.0	17.2	2852	8

Table 5.31

Large Scale PCR Reactor Results

5.4.3 10 ml Run

The first product run was conducted using a 10 ml master mix, run on 19JUN06. Once set points were reached, this master mix was injected at 96°C before the first hold time. The temperature profiles were within declared set points, and were nearly identical to previous buffer runs. It took approximately 90 minutes for the set points to be reached. The reactor continued for an additional 90 minutes of process. Once 90 minutes of process had been reached, the product was pumped into a sterile bottle for analysis. The system was flushed repeatedly with DI water to ensure it would be clean for the next run.

Upon analysis, it was determined that no viable DNA could be detected. It was decided to conduct a run with a higher concentration of master mix.

5.4.4 100 ml Run

The second product run was conducted using a 100 ml master mix, run on 18JUL06. Since this volume could not be injected in process due to the capacity of the bubble trap, the master mix was pumped in along with the buffer. The temperature profiles were within setpoints, and were consistent with earlier runs. After approximately 60 minutes, all of the setpoints were in range. The reactor continued for 50 minutes.
Once process was complete, the product was pumped into a sterile bottle for analysis. The system was flushed repeatedly with DI water to ensure it would be clean for the next run.

Upon analysis, it was determined that no viable DNA could be detected.

5.4.5 Shear Testing

Since no DNA was detected after both of the above runs, a test was conducted to determine if shear forces were destroying the DNA present in the master mix.
Linearized DNA was introduced into the system, with the same buffer solution as the product runs. The loop was run, without the heat exchangers active, for approximately 45 minutes. The solution was pumped into a sterile bottle upon completion.

After testing, it was determined that there was very little degradation of the DNA due to the shear stresses produced by the continuous flow.

5.4.6 Thermal Shock Testing

Due to the large temperature ramp rate of the heat exchangers, a test similar to the shear test was conducted with the heat exchangers active. Since the reactor has such large ramp rates, it was theorized that a form of thermal shock could be degrading or destroying the DNA. Linearized

DNA was introduced into the system, with the same buffer solution as the product runs. The loop was run for approximately 30 minutes. The solution was pumped into a sterile bottle upon completion.

After testing, it was determined that there was very little degradation of the DNA due to thermal shock.

6. 6. Discussion

Since there was no DNA amplification found, this discussion will primarily focus on potential causes of the lack of a PCR reaction.

6.1.1 Anti-foam

A small amount of anti-foam was used in the reaction mix. Anti-foam was deemed necessary due to excessive foaming during runs. The foaming caused incorrect temperature readings. Anti-foam is known to slightly inhibit a PCR reaction.

6.1.2 Hold time set points

Although all hold times were within declared specifications, they were all on the lower end of the time range. For example, hold step two was 10 seconds, and the range was 10-20 seconds. This may not be enough time for the reaction to occur in each hold step.

6.1.3 Ramp rate

The ramp-rate on a PCR thermocycler is 2 °C per second. The ramp rates on the continuous PCR reactor are 100-200 °C per second. It has been shown that the ramp rate itself does not have any affect on the integrity of the product in terms of a fast temperature change. However, the ramp rate may be affecting the timing of the system. In a thermocycler, with a 2 °C ramp rate, there is effectively more hold time due to the time needed for the temperature to increase or decrease. For example, in order for the temperature to go from 72 °C to 96 °C in a thermocycler, it would take 12 seconds. In the continuous PCR reactor, the time to go from 72 °C to 98 °C takes less than a second. Since the hold time specifications after that temperature change is 10-20 seconds, the difference in ramping time could be having a significant effect.

Apppendix II

Vaccination with PCR-generated Linear Expression Cassettes protects Mice against Lethal Influenza A Challenge

Adrián Vilalta[1,2], Gretchen Jimenez, Denis Rusalov[2], Peggy Lalor[2], Kristin Carner[2], Jennifer A. Chaplin[2], Michael Komai[2], Marston Manthorpe[2] and David C. Kaslow[2]

Abbreviations: bp, base pairs; HA, hemagglutinin; pDNA, plasmid DNA; pfu, plaque forming unit; LEC, Linear Expression Cassette; ORF, Open Reading Frame; PCR, Polymerase Chain Reaction; pfu, plaque forming unit

1. Corresponding author. To whom reprint requests should be addressed. E-mail: avilalta@vical.com.
2. Vical Inc., San Diego, CA

Abstract

Feasibility of a Linear Expression Cassette (LEC)-based influenza A DNA vaccine was demonstrated in mice using a lethal dose (LD_{90}) of a mouse-adapted A/Hong Kong/8/68 (H3N2) influenza strain. LECs expressing hemagglutinin (HA) from either the homotypic H3N2 or the heterotypic (A/Puerto Rico/8/34) H1N1 influenza virus were produced using PCR and both phosphodiester and phosphorothioate-modified oligonucleotide primers. Survival to lethal viral challenge was used as a primary endpoint; weight loss was the secondary endpoint. Survival and weight loss data show that full protection can be achieved in mice with 50 μg of PBS-formulated LEC DNA or 2 μg of Vaxfectin™-formulated LEC DNA. Vaccination with a heterotypic H1 LEC DNA provided no protection against viral challenge.

Introduction

Influenza, a highly contagious illness of the respiratory tract, is caused by RNA viruses of the *Orthomyxoviridae* family (Knipe and Howley, 2001). There are three main types of influenza viruses, A, B and C. Structurally, influenza A and B are similar while influenza C presents a different pattern of surface antigens. Major yearly outbreaks of influenza are associated with influenza A or B while infection with type C virus is associated with minor symptoms.

According to the Centers for Disease Control and Prevention (CDC; http://www.cdc.gov/flu/), five to 20% of the United States population gets the flu every year, with about 36,000 deaths annually due to complications from the infection. Influenza and pneumonia are among the top seven leading causes of death in the United States despite over 60 years of licensed influenza vaccine availability; still, the most effective protection against influenza is vaccination. Small periodic changes in the virus surface antigens Hemagglutinin (HA) and Neuroaminidase (NA) require the development of new vaccines every season. Moreover, major changes in HA and NA can result in highly virulent strains that have the potential to cause a pandemic. Outbreaks of influenza in animals increase the chances of a pandemic, through the reassortment of animal and human influenza virus genomes resulting in new virus strains as occurred in the 1957 and 1968 pandemics. Currently, the spread of deadly strains of avian flu virus (H5N1) in birds and the occasional transmission to humans has raised concerns of a potential pandemic and has therefore triggered a re-evaluation of vaccination strategies. It has become clear that successful containment of an outbreak of a highly virulent influenza strain will require fast manufacture of large quantities of vaccines.

Present influenza prevention strategies primarily include the use of antiviral medications and vaccination with the latter being the most cost-effective approach. However, development and manufacture of currently licensed influenza vaccines require the use of outdated technologies that have proven slow and unreliable and are therefore inadequate to meet the challenges of a potentially rapidly changing and spreading pandemic.

Plasmid DNA (pDNA) vaccines have proven effective in a growing number of infectious disease indications in several animal models including mice (Chen *et al.*, 1999; Davis *et al.*, 2001; Margalith and Vilalta, 2006), rabbits (Hermanson *et al.*, 2004), dogs (Lodmell *et al.*, 2003; Bahloul *et al.*, 2006; Lodmell *et al.*, 2006), monkeys (Lodmell *et al.*,

1998), ferrets (Webster *et al.*, 1994), fish (Corbeil *et al.*, 2000; Kurath, 2005) and horses (Davis *et al.*, 2001; Fischer *et al.*, 2003). Currently, pDNA vaccines are being tested for safety and efficacy in humans for a wide range of indications including West Nile Virus, HIV, CMV, SARS, and Ebola amongst others. Recent data indicate that HIV and Ebola pDNA vaccines elicit broad antibody and T-cell responses in human volunteers. Protective responses to influenza A after pDNA vaccination were first reported in 1993 (Montgomery *et al.*, 1993; Robinson *et al.*, 1993; Ulmer *et al.*, 1993). Published data indicate that vaccination with pDNA encoding either Nucleocapsid (NP) (Ulmer *et al.*, 1993), NA (Chen *et al.*, 1999) or HA(Chen *et al.*, 1999) can induce protective responses in mice, although protection might be somewhat dependent on the strain of mice. Reports also indicate that both ferrets and non-human primates can be vaccinated using influenza genes expressed from pDNA (Webster *et al.*, 1994; Donnelly *et al.*, 1995; Donnelly *et al.*, 1997). Although the consensus in the field is that antibody responses to HA are essential for protection from disease(Knipe and Howley, 2001) , inclusion of other antigens such as the highly conserved NP, M1 and M2 proteins could provide protection against antigenic drift variants through the development of cellular immunity.

Ideally, a nucleic acid vaccine could be produced using a cell-free system more akin to a small molecule synthetic process. This approach would avoid bacterial fermentation and the use of antibiotic selection. Moreover, cell-free DNA manufacture would be expected to be faster and more efficient than traditional methods. In the last few years, a new approach to developing DNA vaccines has been proposed. It requires the use of linear DNA (Linear Expression Cassettes; LECs) as opposed to circular pDNA thus avoiding the use of antibiotic resistance genes and other sequences unrelated to the expression of an antigen resulting in the delivery of more copies of the antigen ORF per dose. Other potential advantages of some linear DNA production methods include use of well-defined and simple reactions, ease of purification and therefore, fast vaccine production. Several methods for producing LECs have been described including enzymatic digestion of pDNA (Leutenegger *et al.*, 2000; Schakowski *et al.*, 2001; Moreno *et al.*, 2004) and PCR (Hofman *et al.*, 2001; Johansson *et al.*, 2002; Liang *et al.*, 2002; Xin *et al.*, 2003). LECs have been reported to be expressed both *in vitro* (Schakowski *et al.*, 2001; Liang *et al.*, 2002; Xin *et al.*, 2003) and *in vivo* (Leutenegger *et al.*, 2000; Moreno *et al.*, 2004); their potential as DNA vaccines has been

explored for a few indications including Feline Immunodeficiency Virus (Leutenegger *et al.*, 2000), Hantavirus (Johansson *et al.*, 2002) and Leishmaniasis (Lopez-Fuertes *et al.*, 2002). Potency of LEC DNA vaccines is related to the stability of the nucleic acid towards nucleases (Johansson *et al.*, 2002). Several approaches have been explored in an attempt to increase the stability of linear DNA including using phosphorothioate-modified oligonucleotide primers (Ciafre *et al.*, 1995; Johansson *et al.*, 2002) and ligation of hairpin oligonucleotides to the ends of the linear DNA molecule (Schakowski *et al.*, 2001).

Protection against influenza A disease is believed to require strong humoral responses against HA. Intramuscular injection of pDNA in PBS has been shown to elicit potent cellular but relatively low antibody responses in humans. Therefore, the use of formulations that drive robust B-cell responses would be expected to improve the performance of nucleic acid-based influenza vaccines. Complexation of immunogen-encoding DNA with cationic lipid systems, such as DMRIE-DOPE(San *et al.*, 1993) and Vaxfectin™(Hartikka *et al.*, 2001) offers a potential enhancement to humoral response elicited by DNA in PBS. For instance, Hartikka and co-workers (Hartikka *et al.*, 2001) showed a 20-fold increase in antibody titers against influenza A NP when formulating pDNA with Vaxfectin™ compared to titers obtained with pDNA in PBS. The enhancement of immune responses by Vaxfectin™ formulations is more pronounced when administering low doses of pDNA(Margalith and Vilalta, 2006) which could be translated into significant dose-sparing. Cationic lipid formulations can provide a significant enhancement of protective immune responses as demonstrated by Hermanson and co-workers(Hermanson *et al.*, 2004) who reported the complete protection of rabbits against a lethal dose of aerosolized anthrax spores after immunization with either pDNA-DMRIE-DOPE or pDNA-Vaxfectin™ vaccines.

Data presented here demonstrate that vaccination with influenza A HA-expressing LEC DNA can protect BALB/c mice against a lethal dose of influenza A. LEC DNA was produced through a PCR process using both phosphodiester and phosphorothioate-modified oligonucleotide primers. Unformulated LEC DNA was shown to protect mice against viral challenge. In addition, high levels of protection were observed using lower doses of LEC DNA when formulated with the cationic lipid system Vaxfectin™. PCR amplification can produce LEC DNA within a few hours; purification and formulation of the resulting DNA only required an additional day. In contrast, production of pDNA through conventional

bacterial fermentation followed by cell lysis and chromatography would typically require a minimum of 7 days. Efficacy data as well as ease of manufacture and formulation support further investigation of LEC DNA as a promising alternative to traditional vaccines.

Materials and Methods

PCR amplification of LEC DNA

Oligonucleotide primers (forward 5'TGGCCATTGCATACGTTGTATCCATATCAT and reverse 5' AGTCAGTGAGCGAGGAAGCGGAAGAGTACC) were designed flanking the CMV promoter and the Rabbit Beta Globin (RBG) transcription terminator of Vical's HA expression vector VR10551 such that amplification produces a 3.5 kbp Linear Expression Cassette (LEC) containing CMV promoter/intron and termination sequences in addition to either the influenza A/HK/8/68 H3N2 (H3 HA) or the influenza A/PR/8/34 H1N1 (H1 HA) ORF (Figure 1). Two sets of primers were used (Sigma-Genosys; Saint Louis, MO); the first set was made to contain only standard deoxyribonucleotides while the second set was prepared such that the two 5'-most residues in each primer were derivatized with phosphorothioate (MOD). PCR was carried out using 5 ng of linearized influenza A HA plasmid, 200 μM of each dNTP (Invitrogen; Carlsbad, CA), 2 U of Phusion™ and 1x Phusion™ HF buffer (Finnzymes; Espoo, Finland) in a final volume of 100 μL. PCR was performed in an Applied Biosystems 9700 thermocycler (Foster City, CA) using the following temperature cycling conditions: (a) Un-modified oligonucleotides: 1x 98 °C (30s); 30x [98 °C (15 s), 50 °C (15 s), 72 °C (90 s)]; 1x 72 °C 600 s and (b) MOD oligonucleotides: 1x 98 °C (30s); 35x [98 °C (15 s), 71 °C (15 s), 72 °C (90 s)]; 1x 72 °C 600 s. H3 HA and H1 HA ORFs were cloned at Vical directly from mouse-adapted A/HK/68 H3N2 and A/PR/34 H1N1 strains, respectively.

Purification of Amplification Products

PCR amplification products were purified using DNA-binding resin columns (Qiagen; Valencia, CA) and concentrated using ultrafiltration on Centriplus® columns (Millipore; Bedford, MA). LEC DNA concentration was determined by A_{260} absorption spectrophotometry using at least two dilutions. LEC DNA from several PCR runs was pooled before further testing.

LEC DNA Characterization

LEC DNA was run on Tris-Acetate-EDTA-Ethidium Bromide 1 % agarose gels to confirm the presence of the expected 3.5 kbp band and the absence of unincorporated primers and extraneous DNA bands (Figure 2). DNA lengths were estimated by comparison to 1 kbp

DNA ladder (New England Biolabs; Ipswich, MA). LEC DNA preparations were further characterized by DNA sequence before *in vivo* studies. DNA sequence information was obtained using standard fluorescence-labeled double-stranded dideoxy sequencing technology (Retrogen; San Diego, CA). Sequencing was performed using primers at approximately every 500 bp on both strands. Sequence was assembled using Sequencher™ (Ver 4.1.4, Gene Codes Corporation; Ann Arbor, MI).

In vitro Antigen Expression test

A Western blot assay was used to confirm that H1 HA and H3 HA proteins of the correct immunological specificity and size were expressed from the LECs. Proteins were identified by transfecting mouse melanoma (VM92) cells with LECs, analyzing the cell lysates by Western blot, and verifying that the protein bands were of the expected apparent molecular weight. LECs were transfected into cells at a dose of 1.5 μg/mL complexed with 5 μL/mL ExGen 500 (Fermentas Life Sciences; Burlington, Canada). For positive and negative controls, pDNAs with or without the transgene-specific ORF were transfected into cells at a dose of 3 μg/mL complexed with 10 μL/mL ExGen 500. The cells were harvested 48 hours post-transfection using Versene (Invitrogen; Carlsbad, CA) and lysed with lysis buffer containing 20 mM Tris-HCl, pH 8.0, 300 mM NaCl, 8 mM EDTA, pH 8.0, 10% glycerin, 0.5% NP-40, and one protease inhibitor tablet (Roche; Alameda, CA). Cell lysates were stored at -70 °C prior to Western blot analysis. Samples were analyzed under reducing/denaturing gel electrophoresis conditions in 4-12% Bis-Tris NuPAGE® gels (Invitrogen; Carlsbad, CA). The proteins were transferred to 0.2 μm PVDF membranes (Invitrogen; Carlsbad, CA) and probed with rabbit polyclonal antibodies followed by alkaline-phosphatase conjugated secondary antibodies (Jackson ImmunoResearch; WestGrove, PA). NBT/BCIP substrate (KPL; Gaithersburg, MD) was used to produce visible protein bands.

Formulation

Vaxfectin™ consists of an equimolar mixture of VC1052 ((±)-N- (3-aminopropyl)-N,N-dimethyl-2, 3-bis (myristoleyloxy)-1-propanaminium bromide) and DPyPE (Diphytanoylphosphatidyl-ethanolamine). Preparation of Vaxfectin™ and its formulations were first described by Hartikka and co-workers (Hartikka *et al.*, 2001). Briefly, both VC1052 and DPyPE were resuspended in chloroform, mixed in 1:1 molar ratio, aliquoted

into vials, and dried to create Vaxfectin™ reagent dry lipid film. On the day of injection, the lipid film vials were resuspended in 1 mL 0.9% saline and diluted if necessary. LECs and pDNA were prepared in 0.9% saline, 20 mM sodium phosphate, pH 7.2. DNA (LECs or pDNA) was formulated with Vaxfectin™ by gently streaming the lipid into pDNA of equal volume. All the required doses were prepared by formulating at 0.2 to 0.5 mg/mL range and diluting down to lower concentration as required.

Animal Procedures

All animal procedures were reviewed and approved by Vical's Institutional Animal Care and Use Committee (IACUC), and complied with the standards set forth in the *Guide for the Care and Use of Laboratory Animals* (U.S. Department of Health Services, National Institutes of Health; Bethesda, MD) and the USDA's (Washington, DC) *Animal Welfare Act and Animal Welfare Regulations.*

Vaccination of Rabbits with H3 HA and H1 HA-expressing plasmids

Antibody reagents for HA LEC characterization were obtained through rabbit vaccination. For this purpose, two New Zealand White rabbits (Harlan Sprague-Dawley; Oxford, MI) were vaccinated with Vaxfectin™-formulated H3 HA pDNA. In addition, two rabbits were vaccinated with the Vaxfectin™-formulated H1 HA pDNA. One milligram of pDNA was administered intramuscularly (*rectus femoris*) at 1 mg/mL on days 0, 28 and 56; final bleed was done on day 78 by ear vein puncture.

Immunization of BALB/c mice and Viral Challenge

A mouse-adapted A/HK/8/68 strain was as first described by Ulmer and co-workers (Ulmer *et al.*, 1993). The mouse-adapted virus causes a lethal infection in the majority of mice infected intranasally under ketamine anesthesia at a dilution of 1:10,000 of the viral stock (50 pfu; 1 LD_{90}). At this dose, most of the mice die by day 10 post-challenge. Typically, no more than 20% of naïve mice survive infection at this viral challenge dose. Female BALB/c mice six to eight weeks old (Jackson Laboratories; Bar Harbor, MN) were used for the influenza viral challenge studies. DNA vaccinations were given as bilateral, *rectus femoris* injections followed by intranasal viral challenge at three to six weeks after vaccination. Mice were monitored for survival and weight loss for three weeks following viral challenge. Average weight loss was not calculated for groups that lost 30% or more of the animals.

Statistical Analysis

Mouse weights were analyzed using the Mann-Whitney nonparametric statistical test. Mouse survival was analyzed using a Kaplan-Meier survival plot followed by a log-rank (Mantel-Cox) test. Differences were considered statistically significant when $p \leq 0.05$.

Results

PCR-amplified LEC DNA can protect against Influenza A Lethal Viral Challenge

The feasibility of an LEC DNA-based influenza A vaccine was first determined in mice using a lethal dose of a mouse-adapted virus. The study was designed to test superiority of homotypic H3HA-LEC DNA vaccine versus heterotypic vaccine H1 HA-LEC DNA. Four groups of mice were vaccinated on day 0 and 21 and challenged on day 42 with H3N2 influenza A/HK/8/68 mouse-adapted virus. The groups were: (1) H3 HA-LEC DNA vaccine test (50 μg/dose; 15 mice), (2) H1 HA-LEC DNA vaccine comparator (50 μg/dose; 15 mice), (3) VR4750 H3 HA-pDNA (100 μg/dose; positive control, 10 mice) and (4) PBS, no DNA (15 mice; negative control). The primary study endpoint was survival and the secondary endpoint was weight loss. With 15 mice per test group, this study was 80% powered to test superiority of H3 HA-LEC DNA over H1 HA-LEC DNA. Data from this study are summarized in Figure 3. Mice in both the H3 HA-LEC DNA and H3 HA-pDNA groups survived the lethal virus challenge, did not lose weight or appear ill. In contrast, all of the H1 HA-LEC DNA and PBS -only injected mice lost up to 40% of their body weight and died by day 18.

Low doses of Vaxfectin™-formulated LEC DNA can protect against Influenza Viral Challenge

The efficacy of influenza LEC DNA vaccine was explored in two dose-response studies. In the first study, mice were vaccinated (days 0 and 21; 10 mice per group) with either PBS-formulated H3 HA-LEC DNA (50 μg) or Vaxfectin™-formulated H3 HA-LEC DNA (50 μg) or Vaxfectin™-formulated MOD-H3 HA-LEC DNA (50, 10 and 2 μg). In addition, Vaxfectin™-formulated H3 HA pDNA (100 μg) and PBS groups were included as positive and negative controls, respectively. At the end of the study (nine weeks after first vaccination) all mice in the homotypic (H3 HA) groups survived viral challenge; challenge of mice in the PBS and H1 HA-LEC DNA groups resulted in 10% and 20% survival, respectively. No apparent weight loss was evident for animals in the homotypic vaccine groups except for the 2 μg Vaxfectin™-formulated MOD-H3 HA-LEC DNA where on average a maximum weight loss of about 7% was observed on day 8. All animals in this last group recovered their weight by the end of the study. Animals in the heterotypic (H1 HA) and negative control groups lost up to 25% of their body mass on average with animals

surviving challenge recovering most of their body mass by the end of the study. Survival and body mass data for this study are summarized in Figure 4. Survival at 28 days post-challenge showed statistical significance ($p<0.01$) for H3 HA-LEC DNA and MOD-H3 HA-LEC DNA groups vs. either the PBS control or the H1 HA-LEC DNA.

Single administration of LEC DNA Influenza vaccine can be protective against Influenza Challenge

The second study used the same test and control groups described above for the two administration regimen but mice received only one vaccination on day 0. Viral challenge took place six weeks after vaccination; the study was terminated nine weeks after vaccination. Mice receiving as little as a single 2 μg injection of Vaxfectin™-formulated MOD-H3 HA LEC DNA were 100% protected from H3N2 virus challenge; 40% of mice in the MOD-H1 HA-LEC DNA group and 20% of animals in the PBS-only group survived the viral challenge. Survival and body mass data are presented in Figure 5.

Discussion

Successful response to a pandemic influenza outbreak will require the rapid production of effective vaccines. Current methods of influenza vaccine production rely on slow and outdated technology and are therefore inadequate to meet the demands of an emerging disease outbreak. Due to their ease of production nucleic acid vaccines provide a promising alternative to egg-grown and cell culture-based vaccines. We present data that support the development of an influenza A vaccine based on PCR-generated Linear Expression Cassettes (LECs).

Firstly, we developed PCR conditions that efficiently amplified LECs containing the CMV promoter/intron, a HA ORF and a transcription terminator (Figure 1). In addition to yield, it was considered necessary to use a method that produced DNA with very few mutations. In order to achieve this we used a highly processive and proof-reading thermostable DNA polymerase, i.e., Phusion™. This polymerase is reported to have an error rate of $4.4x10^{-7}$ or about 50-fold lower than *Taq* polymerase. In addition, we used relatively high levels of input template (5 ng) to reduce the chance of mutations occurring in early PCR cycles ("jackpot" mutations) and therefore making a significant proportion of the final product. The use of these amplification conditions was supported by DNA sequence analysis of PCR-amplified LEC DNA (data not shown). Furthermore, the LEC DNA was tested *in vitro* for expression of the HA antigens. Western blot analysis shows the expression of proteins of the expected size and cross-reactivity (Figure 2).

We used lethal doses of a mouse-adapted influenza A/HK/8/68 (H3N2) virus to test the efficacy of LEC DNA vaccination. Our data (Figure 3) indicate that homotypic LEC DNA vaccination fully protects mice when administered at Days 0 and 21 at 50 μg per dose in PBS. Both survival and weight loss data for the homotypic LEC DNA group (H3HA) are indistinguishable from the H3 HA-pDNA positive control. On the other hand, none of the mice in the H1 HA LEC DNA group and PBS groups survived the challenge showing lack of cross strain protection and confirming the lethality of the viral dose used.

Work reported by Johansson and collaborators (Johansson *et al.*, 2002) suggested that phosphorothioate modification of PCR-primers could result in enhanced LEC DNA resistance to exonucleases and, consequently, improved vaccine potency. We tried this approach by using oligonucleotide primers where the two 5'-most residues were

phosphorothioates. In addition, we formulated the resulting LEC DNA (MOD-LECs) with Vaxfectin™ to benefit from the adjuvant effects (Hartikka *et al.*, 2001; Hermanson *et al.*, 2004; Margalith and Vilalta, 2006) of this cationic lipid system. We vaccinated mice with the Vaxfectin™-formulated MOD-LEC DNA using doses ranging from 50 μg to 2 μg. Moreover, we tested the efficacy of vaccination using a single dose of the Vaxfectin™-formulated MOD-LEC DNA. Survival and weight loss data (Figure 4) indicate that two administrations of the LEC vaccine completely protect mice from the viral challenge. Remarkably, a single administration of the LEC DNA H3 HA vaccine at the lowest dose tested (2 μg) was sufficient to confer protection to viral challenge. Mice appeared active and healthy; the only indication of disease in this group was a slight (<10%), non-statistically significant, decrease in average body mass by day 9. All the animals in this group recovered their weight by the end of the study.

Our data therefore demonstrate the feasibility of linear DNA-based vaccines to protect against a lethal dose of influenza A virus. Efficacy of Vaxfectin™-formulated LECs at low doses is consistent with previously published data showing enhanced immune responses of cationic lipid-formulated DNA. Efficacy and ease of manufacture support further development of LEC DNA-based influenza vaccines as a promising approach to rapid vaccine development.

Acknowledgements

This study was partially funded by DARPA grant W911NF-05-1-0545. We thank Drs. Alain Rolland and Larry Smith for critical review of the manuscript. We are also grateful for input from Steve Petersen, Keith Hall, Pamela Resch and Alan Engbring. We appreciate the invaluable technical support from Rod Planchon, David Kurniadi, Jane Morrow, Sylvia Salapski and Melissa Masters.

Author Disclosure Statement

All authors were employees of Vical Inc. at the time the research was conducted. GJ and DCK left Vical Inc. before submission of this manuscript.

References

BAHLOUL, C., TAIEB, D., DIOUANI, M.F., AHMED, S.B., CHTOUROU, Y., B'CHIR B, I., KHARMACHI, H., and DELLAGI, K. (2006). Field trials of a very potent rabies DNA vaccine which induced long lasting virus neutralizing antibodies and protection in dogs in experimental conditions. Vaccine **24**, 1063-1072.

CHEN, Z., YOSHIKAWA, T., KADOWAKI, S., HAGIWARA, Y., MATSUO, K., ASANUMA, H., AIZAWA, C., KURATA, T., and TAMURA, S. (1999). Protection and antibody responses in different strains of mouse immunized with plasmid DNAs encoding influenza virus haemagglutinin, neuraminidase and nucleoprotein. J Gen Virol **80 (Pt 10)**, 2559-2564.

CIAFRE, S.A., RINALDI, M., GASPARINI, P., SERIPA, D., BISCEGLIA, L., ZELANTE, L., FARACE, M.G., and FAZIO, V.M. (1995). Stability and functional effectiveness of phosphorothioate modified duplex DNA and synthetic 'mini-genes'. Nucleic Acids Res **23**, 4134-4142.

CORBEIL, S., KURATH, G., and LAPATRA, S.E. (2000). Fish DNA vaccine against infectious hematopoietic necrosis virus: efficacy of various routes of immunisation. Fish Shellfish Immunol **10**, 711-723.

DAVIS, B.S., CHANG, G.J., CROPP, B., ROEHRIG, J.T., MARTIN, D.A., MITCHELL, C.J., BOWEN, R., and BUNNING, M.L. (2001). West Nile virus recombinant DNA vaccine protects mouse and horse from virus challenge and expresses in vitro a noninfectious recombinant antigen that can be used in enzyme-linked immunosorbent assays. J Virol **75**, 4040-4047.

DONNELLY, J.J., FRIEDMAN, A., MARTINEZ, D., MONTGOMERY, D.L., SHIVER, J.W., MOTZEL, S.L., ULMER, J.B., and LIU, M.A. (1995). Preclinical efficacy of a prototype DNA vaccine: enhanced protection against antigenic drift in influenza virus. Nat Med **1**, 583-587.

DONNELLY, J.J., FRIEDMAN, A., ULMER, J.B., and LIU, M.A. (1997). Further protection against antigenic drift of influenza virus in a ferret model by DNA vaccination. Vaccine **15**, 865-868.

FISCHER, L., MINKE, J., DUFAY, N., BAUDU, P., and AUDONNET, J.C. (2003). Rabies DNA vaccine in the horse: strategies to improve serological responses. Vaccine **21**, 4593-4596.

HARTIKKA, J., BOZOUKOVA, V., FERRARI, M., SUKHU, L., ENAS, J., SAWDEY, M., WLOCH, M.K., TONSKY, K., NORMAN, J., MANTHORPE, M., and WHEELER, C.J. (2001). Vaxfectin enhances the humoral immune response to plasmid DNA-encoded antigens. Vaccine **19**, 1911-1923.

HERMANSON, G., WHITLOW, V., PARKER, S., TONSKY, K., RUSALOV, D., FERRARI, M., LALOR, P., KOMAI, M., MERE, R., BELL, M., BRENNEMAN, K., MATECZUN, A., EVANS, T., KASLOW, D., GALLOWAY, D., and HOBART, P. (2004). A cationic lipid-formulated plasmid DNA vaccine confers sustained antibody-mediated protection against aerosolized anthrax spores. Proc Natl Acad Sci U S A **101**, 13601-13606.

HOFMAN, C.R., DILEO, J.P., LI, Z., LI, S., and HUANG, L. (2001). Efficient in vivo gene transfer by PCR amplified fragment with reduced inflammatory activity. Gene Ther **8**, 71-74.

JOHANSSON, P., LINDGREN, T., LUNDSTROM, M., HOLMSTROM, A., ELGH, F., and BUCHT, G. (2002). PCR-generated linear DNA fragments utilized as a hantavirus DNA vaccine. Vaccine **20**, 3379-3388.

KNIPE, D.M., and HOWLEY, P.M. (2001). *Fields Virology*. (Lippincott Williams and Wilkins, Philadelphia).

KURATH, G. (2005). Overview of recent DNA vaccine development for fish. Dev Biol (Basel) **121**, 201-213.

LEUTENEGGER, C.M., BORETTI, F.S., MISLIN, C.N., FLYNN, J.N., SCHROFF, M., HABEL, A., JUNGHANS, C., KOENIG-MEREDIZ, S.A., SIGRIST, B., AUBERT, A., PEDERSEN, N.C., WITTIG, B., and LUTZ, H. (2000). Immunization of cats against feline immunodeficiency virus (FIV) infection by using minimalistic immunogenic defined gene expression vector vaccines expressing FIV gp140 alone or with feline interleukin-12 (IL-12), IL-16, or a CpG motif. J Virol **74**, 10447-10457.

LIANG, X., TENG, A., BRAUN, D.M., FELGNER, J., WANG, Y., BAKER, S.I., CHEN, S., ZELPHATI, O., and FELGNER, P.L. (2002). Transcriptionally active polymerase chain reaction (TAP): high throughput gene expression using genome sequence data. J Biol Chem **277**, 3593-3598.

LODMELL, D.L., EWALT, L.C., PARNELL, M.J., RUPPRECHT, C.E., and HANLON, C.A. (2006). One-time intradermal DNA vaccination in ear pinnae one year prior to infection protects dogs against rabies virus. Vaccine **24**, 412-416.

LODMELL, D.L., PARNELL, M.J., WEYHRICH, J.T., and EWALT, L.C. (2003). Canine rabies DNA vaccination: a single-dose intradermal injection into ear pinnae elicits elevated and persistent levels of neutralizing antibody. Vaccine **21**, 3998-4002.

LODMELL, D.L., RAY, N.B., PARNELL, M.J., EWALT, L.C., HANLON, C.A., SHADDOCK, J.H., SANDERLIN, D.S., and RUPPRECHT, C.E. (1998). DNA immunization protects nonhuman primates against rabies virus. Nat Med **4**, 949-952.

LOPEZ-FUERTES, L., PEREZ-JIMENEZ, E., VILA-CORO, A.J., SACK, F., MORENO, S., KONIG, S.A., JUNGHANS, C., WITTIG, B., TIMON, M., and ESTEBAN, M. (2002). DNA vaccination with linear minimalistic (MIDGE) vectors confers protection against Leishmania major infection in mice. Vaccine **21**, 247-257.

MARGALITH, M., and VILALTA, A. (2006). Sustained protective rabies neutralizing antibody titers after administration of cationic lipid-formulated pDNA vaccine. Genet Vaccines Ther **4**, 2.

MONTGOMERY, D.L., SHIVER, J.W., LEANDER, K.R., PERRY, H.C., FRIEDMAN, A., MARTINEZ, D., ULMER, J.B., DONNELLY, J.J., and LIU, M.A. (1993). Heterologous and homologous protection against influenza A by DNA vaccination: optimization of DNA vectors. DNA Cell Biol **12**, 777-783.

MORENO, S., LOPEZ-FUERTES, L., VILA-CORO, A.J., SACK, F., SMITH, C.A., KONIG, S.A., WITTIG, B., SCHROFF, M., JUHLS, C., JUNGHANS, C., and TIMON, M. (2004). DNA immunisation with minimalistic expression constructs. Vaccine **22**, 1709-1716.

ROBINSON, H.L., HUNT, L.A., and WEBSTER, R.G. (1993). Protection against a lethal influenza virus challenge by immunization with a haemagglutinin-expressing plasmid DNA. Vaccine **11**, 957-960.

SAN, H., YANG, Z.Y., POMPILI, V.J., JAFFE, M.L., PLAUTZ, G.E., XU, L., FELGNER, J.H., WHEELER, C.J., FELGNER, P.L., GAO, X., and ET AL. (1993). Safety and

short-term toxicity of a novel cationic lipid formulation for human gene therapy. Hum Gene Ther **4**, 781-788.

SCHAKOWSKI, F., GORSCHLUTER, M., JUNGHANS, C., SCHROFF, M., BUTTGEREIT, P., ZISKE, C., SCHOTTKER, B., KONIG-MEREDIZ, S.A., SAUERBRUCH, T., WITTIG, B., and SCHMIDT-WOLF, I.G. (2001). A novel minimal-size vector (MIDGE) improves transgene expression in colon carcinoma cells and avoids transfection of undesired DNA. Mol Ther **3**, 793-800.

ULMER, J.B., DONNELLY, J.J., PARKER, S.E., RHODES, G.H., FELGNER, P.L., DWARKI, V.J., GROMKOWSKI, S.H., DECK, R.R., DEWITT, C.M., FRIEDMAN, A., and ET AL. (1993). Heterologous protection against influenza by injection of DNA encoding a viral protein. Science **259**, 1745-1749.

WEBSTER, R.G., FYNAN, E.F., SANTORO, J.C., and ROBINSON, H. (1994). Protection of ferrets against influenza challenge with a DNA vaccine to the haemagglutinin. Vaccine **12**, 1495-1498.

XIN, W., MA, J., and HUANG, D.W. (2003). Assembly of linear functional expression elements with DNA fragments digested with asymmetric restriction endonucleases. Biotechnol Lett **25**, 901-904.

Figure Legends

Figure 1. Linear Expression Cassette. PCR-generated linear DNA is shown in relation to the linearized pDNA template. Expression cassette contains the human CMV promoter and intron A, the influenza A hemagglutinin (HA) ORF and the Rabbit Beta Globin (RBG) terminator. Kanamycin resistance (Kan^r) gene in the pDNA template is also indicated.

Figure 2. *In vitro* characterization of LECs. (A) Representative agarose gel depicting H3 HA and H1 HA LECs. Lane 1 H3 HA-LEC, lane 2 MOD-H3 HA-LEC, lane 3 H1 HA-LEC, lane 4 MOD-H1 HA-LEC, lanes labeled M contain DNA ladder; **(B)** *in vitro* expression of LECs and MOD-LEC was tested by transfecting mouse melanoma (VM92) cells with LECs followed by Western blot analysis of cell lysates as described in Materials and Methods. Lanes 1 and 11, empty pDNA vector; lanes 2, 9, 12 and 19, M_r marker; lanes 4, 6, 8, 13, 15 and 17 are empty; lanes 10 and 20, un-transfected VM92 cells. For H3HA, lane3, MOD-LEC; lane 5, LEC; lane 7, pDNA. For H1HA, lane 14, MOD-LEC; lane 16, LEC; lane 18, pDNA. Cross-reacting HA bands are indicated with an arrow.

Figure 3. Vaccination with PBS-formulated LEC. Mice (15 mice per group) were vaccinated on Days 0 and 21 with either 50 μg of H3HA-LEC or H1HA-LEC; H3HA-pDNA (100 μg) and PBS-only groups were included as positive and negative controls, respectively. Mice were challenged with a lethal dose (LD_{90}) of a mouse-adapted Influenza A/HK/8/68 (H3N2) on day 42 as described in Materials and Methods. Survival data are presented in **(A)**; average group weights are shown in **(B)**.

Figure 4. Vaccination with Vaxfectin™-formulated LEC. Mice were vaccinated on days 0 and 21 with either PBS-formulated H3HA-LEC (50 μg) or Vaxfectin™-formulated H3 HA-LEC (50 μg) or Vaxfectin™-formulated MOD-H3 HA-LEC (50, 10 and 2 μg). In addition, Vaxfectin™-formulated H3 HA pDNA (100 μg) and PBS groups were included as positive and negative control, respectively. Mice were challenged with 1 LD_{90} of a mouse-adapted Influenza A/HK/8/68 (H3N2) on day 42 as described in Materials and Methods. Survival data are presented in **(A)**; average group weights are shown in **(B)**.

Figure 5. Single administration of Vaxfectin™-formulated LEC. LEC vaccine was administered on day 0; mice were challenged on day 42 as described in Materials and Methods. Groups included PBS-formulated H3HA-LEC (50 μg) or Vaxfectin™-formulated

H3 HA-LEC (50 μg) or Vaxfectin™-formulated MOD-H3 HA-LEC (50, 10 and 2 μg). In addition, Vaxfectin™-formulated H3 HA pDNA (100 μg) and PBS groups were included as positive and negative controls, respectively. Survival and weight data are presented in **(A)** and **(B)**, respectively.

Figure 1

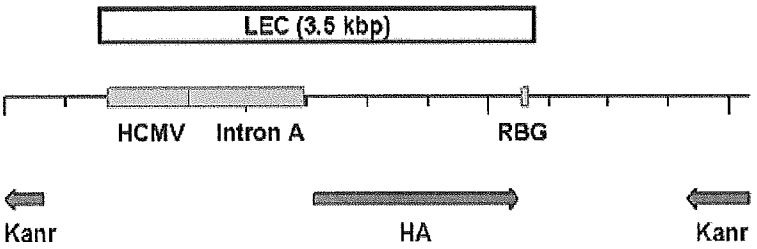

Figure 2.

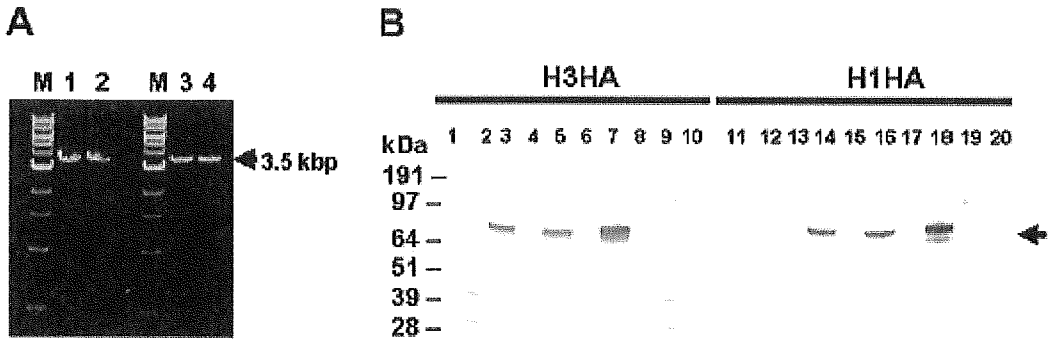
A
M 1 2 M 3 4
3.5 kbp
B
H3HA
H1HA
kDa
1 2 3 4 5 6 7 8 9 10 11 12 13 14 15 16 17 18 19 20
191 –
97 –
64 –
51 –
39 –
28 –

Figure 3.

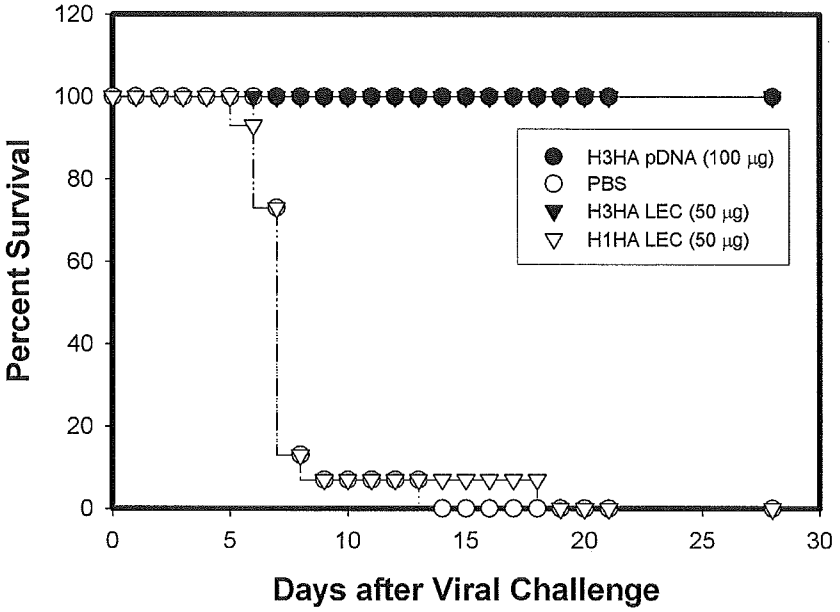
Percent Survival
Days after Viral Challenge
H3HA pDNA (100 μg)
PBS
H3HA LEC (50 μg)
H1HA LEC (50 μg)

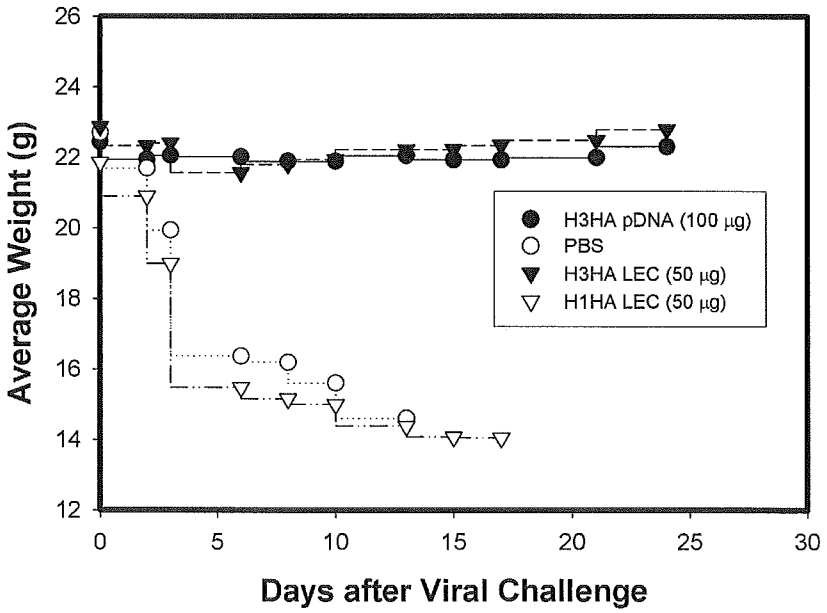
Average Weight (g)
Days after Viral Challenge
H3HA pDNA (100 μg)
PBS
H3HA LEC (50 μg)
H1HA LEC (50 μg)

Figure 4.

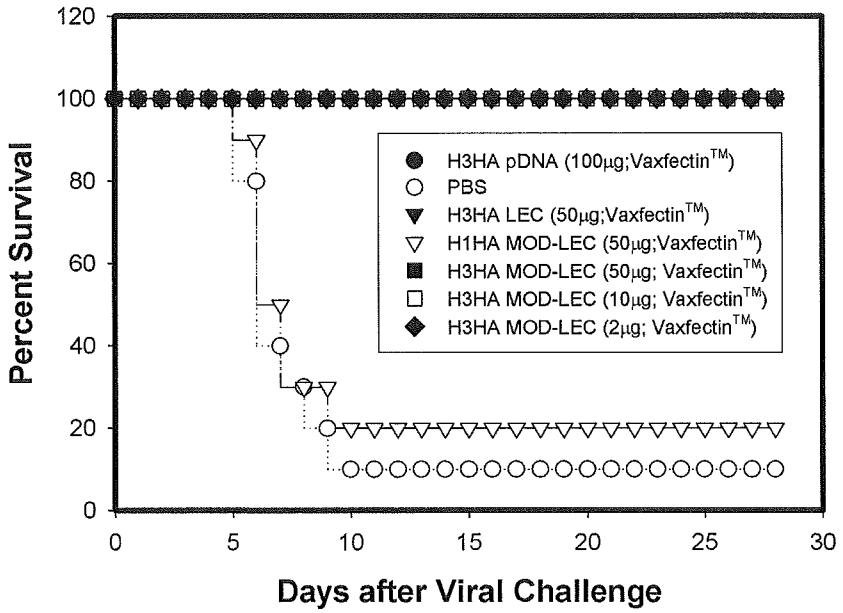
Percent Survival
120
100
80
60
40
20
0
0
5
10
15
20
25
30
Days after Viral Challenge
H3HA pDNA (100μg;Vaxfectin™)
PBS
H3HA LEC (50μg;Vaxfectin™)
H1HA MOD-LEC (50μg;Vaxfectin™)
H3HA MOD-LEC (50μg; Vaxfectin™)
H3HA MOD-LEC (10μg; Vaxfectin™)
H3HA MOD-LEC (2μg; Vaxfectin™)

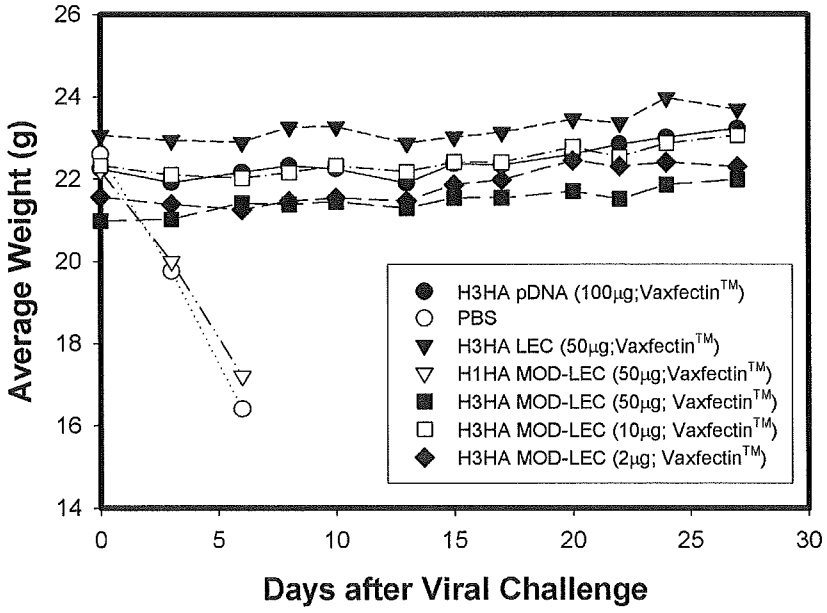
Average Weight (g)
26
24
22
20
18
16
14
0
5
10
15
20
25
30
Days after Viral Challenge
H3HA pDNA (100μg;Vaxfectin™)
PBS
H3HA LEC (50μg;Vaxfectin™)
H1HA MOD-LEC (50μg;Vaxfectin™)
H3HA MOD-LEC (50μg; Vaxfectin™)
H3HA MOD-LEC (10μg; Vaxfectin™)
H3HA MOD-LEC (2μg; Vaxfectin™)

Figure 5.

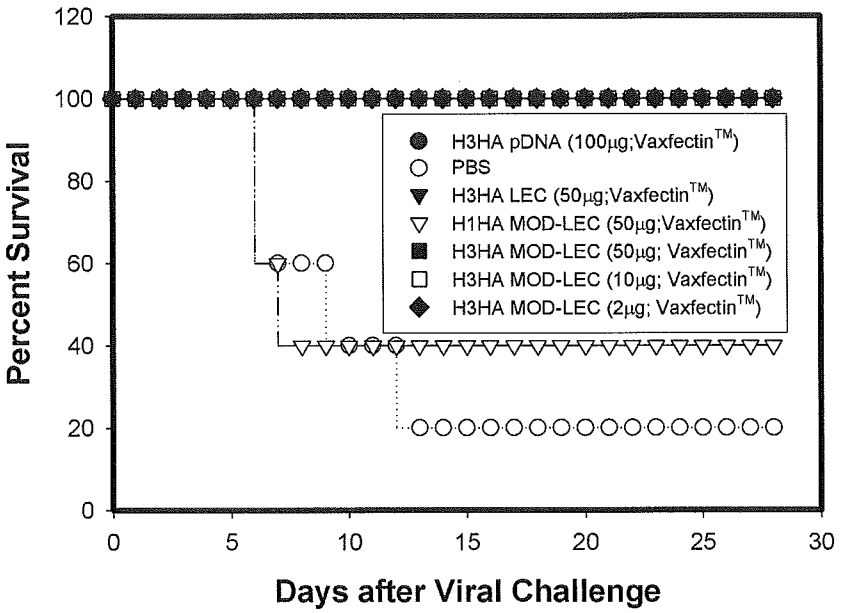
Percent Survival
Days after Viral Challenge
H3HA pDNA (100μg;Vaxfectin™)
PBS
H3HA LEC (50μg;Vaxfectin™)
H1HA MOD-LEC (50μg;Vaxfectin™)
H3HA MOD-LEC (50μg; Vaxfectin™)
H3HA MOD-LEC (10μg; Vaxfectin™)
H3HA MOD-LEC (2μg; Vaxfectin™)

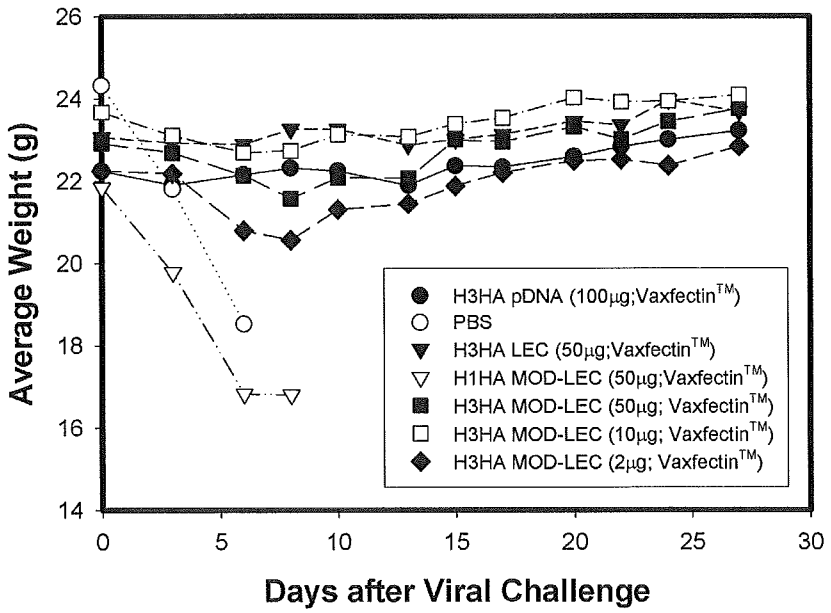
Average Weight (g)
Days after Viral Challenge
H3HA pDNA (100μg;Vaxfectin™)
PBS
H3HA LEC (50μg;Vaxfectin™)
H1HA MOD-LEC (50μg;Vaxfectin™)
H3HA MOD-LEC (50μg; Vaxfectin™)
H3HA MOD-LEC (10μg; Vaxfectin™)
H3HA MOD-LEC (2μg; Vaxfectin™)